Mass spectrum of 2-dimensional $\mathcal{N} = (2,2)$ super Yang-Mills theory on the lattice

D. August, M. Steinhauser, B.H. Wellegehausen and A. Wipf

Theoretisch-Physikalisches Institut, Friedrich-Schiller University Jena,
Max-Wien-Platz 1, 07743 Jena, Germany

E-mail: daniel.august@uni-jena.de, marc.steinhauser@uni-jena.de,
bjoern.wellegehausen@uni-jena.de, wipf@tpi.uni-jena.de

ABSTRACT: In the present work we analyse $\mathcal{N} = (2,2)$ supersymmetric Yang-Mills (SYM) theory with gauge group SU(2) in two dimensions by means of lattice simulations. The theory arises as dimensional reduction of $\mathcal{N} = 1$ SYM theory in four dimensions. As in other gauge theories with extended supersymmetry, the classical scalar potential has flat directions which may destabilize numerical simulations. In addition, the fermion determinant need not be positive and this sign-problem may cause further problems in a stochastic treatment. We demonstrate that $\mathcal{N} = (2,2)$ super Yang-Mills theory has actually no sign problem and that the flat directions are lifted and thus stabilized by quantum corrections. Only the bare masses of the scalars experience a finite additive renormalization in this finite theory. On various lattices with different lattice constants we determine the scalar masses and hopping parameters for which the supersymmetry violating terms are minimal. By studying four Ward identities and by monitoring the π-mass we show that supersymmetry is indeed restored in the continuum limit. In the second part we calculate the masses of the low-lying bound states. We find that in the infinite-volume and supersymmetric continuum limit the Veneziano-Yankielowicz super-multiplet becomes massless and the Farrar-Gabadadze-Schwetz super-multiplet decouples from the theory. In addition, we estimate the masses of the excited mesons in the Veneziano-Yankielowicz multiplet. We observe that the gluino-glueballs have comparable masses to the excited mesons.

Contents

1 Introduction

Many extensions of the standard model of particle physics make use of supersymmetry in order to cure well-known flaws of the standard model, as for instance the hierarchy problem. Some of the additional particles of supersymmetric (susy) gauge theories may be identified as dark matter particles in the universe. Since no additional particles have been observed in experiments up to now it is of utmost interest to investigate the spectrum of susy gauge theories, in particular in the strongly coupled regime. The most simple supersymmetric gauge theories are probably the $\mathcal{N} = 1$ Super-Yang-Mills (SYM) theories

with gauge groups SU(N). These are supersymmetric extensions of SU(N) Yang-Mills theories [1, 2]. For SU(3) the bosonic sector is identical to that of QCD. It describes the gluons of strong interaction in interaction with their superpartners, the gluinos. The gluinos are Majorana fermions transforming in the adjoint representation of the gauge group. Like in QCD, the theory is asymptotically free and it is expected, that the gluons and gluinos are confined in colorless bound states. But differently from one-flavor QCD, the U(1)$_A$ chiral symmetry is anomalously broken only to the discrete subgroup $\mathbb{Z}_{2N}$. At low temperatures this symmetry is further broken spontaneously to $\mathbb{Z}_2$ by the formation of a gluino condensate and thus gives rise to N physically equivalent vacua [3].

The SYM theory has a richer spectrum of colour-blind bound states than QCD since the gluinos are in the adjoint representation. Beside (adjoint) mesons, baryons and glueballs, hybrid bound states of gluons and gluinos are expected to show up in the low energy spectrum. Implementing symmetries and anomalies of the theory, low energy effective actions have been proposed [4–6] describing the supersymmetric spectrum of bound states. Thereby the chiral multiplet containing the adjoint f- and η-meson is extended to a super-multiplet by a gluino-glueball. A second multiplet contains a 0^+ glueball, a 0^- glueball and in addition a gluino-glueball. The low-energy effective action depends on free parameters and hence it is not clear which multiplet is the lighter one. Various arguments were given for both scenarios, see [4–7]. Another difficulty stems from the fact, that for every state in the first multiplet there exists a state in the second multiplet with the same quantum numbers. This mixing of states may lead to an even more complex multiplet structure.

Similarly as QCD the $\mathcal{N} = 1$ SYM theory is strongly coupled at low energies and non-perturbative methods are necessary to investigate its mass spectrum. We simulate the theory on a discrete spacetime lattice. This is a non-trivial task since a lattice regularisation breaks supersymmetry explicitly. This can be seen from the susy algebra

$$\{\mathcal{Q}, \mathcal{Q}\} \propto P_\mu,$$

where $\mathcal{Q}$ is a generator of supersymmetry and the P_μ generate translations in space and time. Since a discrete lattice does not admit arbitrary small translations, we can not preserve the full supersymmetry on a lattice, similar to chiral symmetry. In order to recover both symmetries in the continuum limit, certain parameters have to be fine-tuned, making simulations more expensive. Fortunately for $\mathcal{N} = 1$ SYM theory, the only relevant operator that breaks supersymmetry (softly) is a non-vanishing gluino condensate which at the same time breaks chiral symmetry. Thus it suffices to restore chiral symmetry in the continuum limit to recover supersymmetry [8], making chiral Ginsparg-Wilson fermions the preferred choice [9–11]. Unfortunately chiral fermions are computationally very expensive such that it seems to be more efficient to fine-tune the bare gluino mass parameter of Wilson fermions. For the gauge group SU(2) with Wilson fermions, the theory has been extensively investigated by the DESY-Münster collaboration [12–19]. Their results confirm the formation of the predicted super-multiplets and reveal, that the glueballs are heavier than the mesons. Simulations for the gauge group SU(3) are underway [20, 21].

Another strategy is to look at the dimensionally reduced model, namely $\mathcal{N} = (2, 2)$ SYM theory in two dimensions. By calculating the mass spectrum of this related and

simpler model we should get further insights into the four-dimensional model. The two-dimensional super-renormalizable descendant of the four-dimensional theory allows for larger lattices and much better statistics. This will lead to a mass spectrum with less statistical errors than in four dimensions.

A first numerical simulation of the two-dimensional model was presented in [22, 23], where the dimensional reduction was done for the lattice theory with compact link variables. Accordingly the scalar fields in the reduced model appear in the exponent of the compact link variables. In the simulation the quenched configurations were reweighted with the Pfaffian. Because of large (statistical) errors the results for Ward identities were inconclusive.

Apart from being a descendant of SYM theory in four dimensions, the $\mathcal{N} = (2,2)$ theory in two dimensions has further interesting properties. Theoretical arguments [24, 25] and numerical calculations based on a discretized light cone quantization [26, 27], both suggest massless states in the physical spectrum. This massless super-multiplet is not seen in four dimensions. Furthermore, it has been conjectured that dynamical susy breaking may occur in the theory [28]. Recent lattice results for the vacuum energy however show no sign of susy breaking [29].

Analogous to the two-dimensional $\mathcal{N} = (2,2)$ Wess-Zumino model [30], the two-dimensional $\mathcal{N} = (2,2)$ SYM theory admits a conserved and nilpotent supercharge. This is possible because there are four supercharges from which one can build *one* nilpotent supercharge $\mathcal{Q}$. On a lattice only the subalgebra generated by nilpotent supercharges can be realized. Several $\mathcal{Q}$-exact lattice models were proposed [31–33]. All these models suffer from the following problem: usually one can expand the link variables as $U_\mu = \mathbb{1} + \mathrm{i}aA_\mu + \cdots$, in which case we expect an unique vacuum state. This is not the case in all three models proposed and thus one expects an ambiguous continuum limit. In the models in [31, 32] the problem is solved by adding the susy-breaking term $\mu^2 \, \mathrm{tr} \left(U^\dagger U - \mathbb{1} \right)^2$ to the Lagrangian, which dynamically picks a unique vacuum state. In the limit $\mu \to 0$, supersymmetry is recovered in this construction. In contrast, by deforming the model [33] the unphysical vacuum states can be removed without breaking the nilpotent supersymmetry explicitly [34]. Several numerical investigations show the restoration of the full susy (not only the nilpotent one) [35–41]. The relations between these models were investigated in [42–45]. For a more detailed overview see the reviews [46–50].

Two-dimensional continuum gauge theories have less dynamical degrees of freedom than four-dimensional ones and thus we may expect that topology of the (Euclidean) spacetime becomes more important. In our work we use periodic lattices which discretize a two-torus. In the works [51–53] different lattices with other spacetimes were scrutinized. In particular a generalized topological twisting on generic Riemann surfaces in two dimensions [51] has been considered. The authors revealed the connection of the sign problem, which is absent on the torus, to the U(1)$_A$ anomaly. With a so called compensator the sign problem can be solved on Riemann surfaces with genus $\neq 1$. Ward identities and the U(1)$_A$ anomaly — the latter is intimately related to the zero modes of the Dirac operator — have been looked at.

The paper is organized as follows: in section 2 we introduce the $\mathcal{N} = (2,2)$ theory, discuss its continuum properties and in particular the expected particle spectrum. There is

only one relevant operator $\text{tr}\,\phi^2$ that needs to be fine-tuned to recover susy in the continuum limit. The corresponding mass-parameter is calculated to one-loop order. To investigate the restoration of susy we derive three independent Ward identities. In section 3 we introduce our lattice formulation with Wilson fermions and discuss some technical points like the fermion sign problem, potentially flat directions of the effective potential and fine-tuning of the bare parameters. In [54, 55] it was argued that it is important to control flat directions of the scalar potential. We shall see in our simulations that the flat directions are lifted and we observe no instabilities in the scalar subsector. Furthermore the model has no sign problem in the simulations. Since susy is broken at finite lattice spacing, the Ward identities are not fulfilled. The additional contributions at finite lattice spacing are discussed in section 4 for the gauge group SU(2), together with our simulation results concerning the restoration of supersymmetry in the continuum and thermodynamic limit. In section 5 we present our accurate results for the masses of the low lying bound states. One super-multiplet becomes massless in the thermodynamic and supersymmetric limit and a second super-multiplet decouples from the theory. In addition we see a massive super-multiplet of excited states. At the end we present our conclusions in section 6.

2 $\mathcal{N} = (2, 2)$ SYM theory in two dimensions

In this section we will derive $\mathcal{N} = (2, 2)$ supersymmetric Yang-Mills (SYM) theory in two dimensions by a dimensional torus-reduction from $\mathcal{N} = 1$ SYM theory in four dimensions. To recall this reduction is useful since there is a one-to-one correspondence between the $\mathcal{N} = 1$ super-multiplets in four dimensions and the $\mathcal{N} = (2, 2)$ super-multiplets in two dimensions. We expect that related super-multiplets have the same length since the length can only change when supersymmetry is (partially) broken or the members of a super-multiplet become massless. Thus we may expect that bound states in the two-dimensional theory arrange in super-multiplets corresponding to super-multiplets in the four-dimensional theory. Note that the assignment of spins in a super-multiplet may change during the reduction. This happens for the vector super-multiplet but not for the chiral super-multiplet. But the mass spectrum may change, even if there is a one-to-one assignment of super-multiplets.

We begin with reviewing some relevant properties of the four-dimensional theory [1, 2]. The action is given by

$$S = \int \mathrm{d}^4 x \, \text{tr} \left(-\frac{1}{4} F_{MN} F^{MN} + \frac{\mathrm{i}}{2} \bar{\lambda} \, \Gamma^M D_M \lambda \right), \tag{2.1}$$

where capital indices M, N assume the values $0, 1, 2, 3$, the matrices Γ^M build an irreducible representation of the four-dimensional Clifford algebra and F_{MN} is the field strength tensor

$$F_{MN} = \partial_M A_N - \partial_N A_M - \mathrm{i}\, g \, [A_M, A_N] \tag{2.2}$$

with gauge potential A_M in the adjoint representation of the gauge group SU(N). The gauge potential and Majorana-field are components of the same super-field such that λ transforms under the adjoint representation as well. Hence, the covariant derivative of the Majorana fermion is

$$D_M \lambda = \partial_M \lambda - \mathrm{i}\, g \, [A_M, \lambda]. \tag{2.3}$$

The action (2.1) is invariant under the on-shell supersymmetry transformations

$$\delta_\varepsilon A_\mu = \mathrm{i}\bar\varepsilon\,\Gamma_M\lambda,\ \ \delta_\varepsilon\lambda = \mathrm{i}F^{MN}\Sigma_{MN}\,\varepsilon,\ \ \delta_\varepsilon\bar\lambda = -\mathrm{i}\bar\varepsilon\,F^{MN}\Sigma_{MN} \tag{2.4}$$

with $[\Gamma_M,\Gamma_N] = 4\mathrm{i}\,\Sigma_{MN}$. These transformations are generated by $\bar\varepsilon Q$, where ε is a constant anticommuting Majorana-valued parameter and the $\{Q^\alpha\}$ are the four components of the Majorana-valued supercharge Q. The Majorana condition relates the four entries of a spinor according to $\lambda = \lambda_c = \mathcal{C}\bar\lambda^\mathsf{T}$, where $\mathcal{C}$ is a charge conjugation matrix.

The action is also invariant under global $\mathrm{U}(1)_A$ transformations

$$\lambda \to e^{\mathrm{i}\alpha\,\Gamma_5}\lambda, \qquad \Gamma_5 = \mathrm{i}\,\Gamma^0\Gamma^1\Gamma^2\Gamma^3\,. \tag{2.5}$$

In the quantum theory, this chiral symmetry is broken down to $\mathbb{Z}_{2N}$ via instantons. If a chiral condensate $\langle\bar\lambda\lambda\rangle \neq 0$ forms, it is further broken spontaneously to $\mathbb{Z}_2$

$$\mathrm{U}(1)_A \overset{\text{instantons}}{\longrightarrow} \mathbb{Z}_{2N} \overset{\langle\bar\lambda\lambda\rangle}{\to} \mathbb{Z}_2\,. \tag{2.6}$$

The N physically equivalent vacua are related by the discrete chiral rotations

$$\lambda \to \exp\left(\mathrm{i}\frac{2n\pi}{N}\Gamma_5\right)\lambda, \quad n = 0,1,2,\ldots,N-1. \tag{2.7}$$

Lattice simulations of four-dimensional $\mathcal{N} = 1$ SYM show that chiral symmetry is indeed spontaneously broken at zero temperature and restored above a critical temperature [17].

The two-dimensional $\mathcal{N} = (2,2)$ SYM theory can be derived from the four-dimensional theory via a Kaluza-Klein torus reduction. Thereby one compactifies two directions on a torus such that $\mathbb{R}^4 \to \mathbb{R}^2 \times \mathcal{T}^2$ and assumes, that the fields are constant on the torus, e.g. $\partial_M\lambda = 0$ for $M = 2,3$. The remaining non-compact coordinates are x^μ with $\mu \in \{0,1\}$. Although the reduction does not depend on the particular representation of the four-dimensional Γ matrices, it is convenient to choose a particular one:

$$\Gamma_\mu = \mathbb{1}\otimes\gamma_\mu, \quad \Gamma_2 = \mathrm{i}\sigma_1\otimes\gamma_5, \quad \Gamma_3 = \mathrm{i}\sigma_3\otimes\gamma_5, \quad \Gamma_5 = \sigma_2\otimes\gamma_5 \tag{2.8}$$

with $\gamma_5 = \gamma_0\gamma_1$. In this representation, the charge conjugation matrices in two and four dimensions are related as $\mathcal{C}_4 = \mathbb{1}\otimes\mathcal{C}_2$ and satisfy

$$\mathcal{C}_2\gamma_\mu\mathcal{C}_2^{-1} = -\gamma_\mu^\mathsf{T} \quad \Longrightarrow \quad \mathcal{C}_4\Gamma_M\mathcal{C}_4^{-1} = -\Gamma_M^\mathsf{T}. \tag{2.9}$$

In a Majorana representation with purely real or imaginary γ_μ we may choose $\mathcal{C}_2 = -\gamma^0$. Applying the dimensional reduction to the Yang-Mills Lagrangian yields

$$-\frac{1}{4}F_{MN}F^{MN} = -\frac{1}{4}F_{\mu\nu}F^{\mu\nu} + \frac{1}{2}D_\mu\phi_m D^\mu\phi_m + \frac{g^2}{4}\left[\phi_m,\phi_n\right]\left[\phi^m,\phi^n\right], \tag{2.10}$$

where the first term on the right hand side is the two-dimensional Yang-Mills Lagrangian, the second term a kinetic term for the two adjoint scalar fields $\phi_m = A_{m+1}$ with $m \in \{1,2\}$ and the third term a quartic interaction potential for the scalar fields. The kinetic term

for the four-dimensional Majorana fermion decomposes in a two-dimensional kinetic part
and a Yukawa interaction between the Majorana fermion λ and the scalar fields ϕ_m,

$$\bar{\lambda}\,\Gamma^M D_M \lambda = \bar{\lambda}\,\Gamma^\mu D_\mu \lambda - \mathrm{i}\,g\bar{\lambda}\,\Gamma^{m+1}\,[\phi_m, \lambda]\,. \tag{2.11}$$

Note, that the four-component Majorana spinor λ turns into two (real) Majorana spinors
in two dimensions (in two dimensions an irreducible spinor has two components only).
Later we will merge them into one complex two-component Dirac spinor. After rescaling
all fields A, λ and ϕ according to $A \to g^{-1}A$ and absorbing afterwards the volume of
the compactified torus in the gauge coupling $1/g^2 \to V_{\mathcal{T}}/g^2$, we obtain the action of the
two-dimensional $\mathcal{N} = (2,2)$ SYM theory

$$
\begin{aligned}
S = \frac{1}{2g^2}\int \mathrm{d}^2x\,\mathrm{tr}\Big\{ &-\frac{1}{2}F_{\mu\nu}F^{\mu\nu} + \mathrm{i}\bar{\lambda}\Gamma^\mu D_\mu \lambda + D_\mu\phi_m D^\mu\phi_m \\
&+\bar{\lambda}\,\Gamma^{m+1}\,[\phi_m, \lambda] + \frac{1}{2}\,[\phi_m, \phi_n]\,[\phi^m, \phi^n]\Big\}\,,
\end{aligned}
\tag{2.12}
$$

the Euclidean version of which we use in our lattice simulations. In a next step we combine
the four components of the Majorana spinor λ in two components of an irreducible Dirac
spinor in two dimensions and rewrite the action in terms of Dirac fermions and complex
scalars. Then the symmetries of the model are transparent and we can easily compare with
the $\mathcal{Q}$-exact formalism [32]. With the ansatz

$$\lambda = \sum_{r=1}^{2} e_r \otimes \chi_r \quad \Longrightarrow \quad \bar{\lambda} = \sum_{r=1}^{2} e_r^{\mathsf{T}} \otimes \bar{\chi}_r\,, \tag{2.13}$$

where $\{e_1, e_2\}$ is a Cartesian basis of $\mathbb{R}^2$, on which Γ^0 in (2.8) acts trivially, and χ_r are
irreducible Majorana spinors in two dimensions, we obtain

$$
\begin{aligned}
S = \frac{1}{2g^2}\int \mathrm{d}^2x\,\mathrm{tr}\Big\{ &-\frac{1}{2}F_{\mu\nu}F^{\mu\nu} + D_\mu\phi_m D^\mu\phi_m + \frac{1}{2}[\phi_m, \phi_n][\phi_m, \phi_n] \\
&+ \mathrm{i}\bar{\chi}_r\gamma^\mu D_\mu \chi_r - \bar{\chi}_r(\mathrm{i}\sigma_1)^{rs}\gamma_5[\phi_1, \chi_s] - \bar{\chi}_r(\mathrm{i}\sigma_3)^{rs}\gamma_5[\phi_2, \chi_s]\Big\}
\end{aligned}
\tag{2.14}
$$

that contains two flavours χ_r of Majorana fermions and two real scalar fields. Introducing
the Dirac fermion ψ and the complex scalar φ according to

$$\psi = \frac{1}{\sqrt{2}}\left(\chi_1 + \mathrm{i}\gamma_5\chi_2\right),\quad \bar{\psi} = \frac{1}{\sqrt{2}}\left(\bar{\chi}_1 + \mathrm{i}\bar{\chi}_2\gamma_5\right),\quad \varphi = \phi_1 + \mathrm{i}\phi_2\,, \tag{2.15}$$

we end up with

$$
\begin{aligned}
S = \frac{1}{g^2}\int \mathrm{d}^2x\,\mathrm{tr}\Big\{ &-\frac{1}{4}F_{\mu\nu}F^{\mu\nu} + \frac{1}{2}(D_\mu\varphi)^\dagger(D^\mu\varphi) - \frac{1}{8}\big[\varphi^\dagger, \varphi\big]^2 \\
&+ \mathrm{i}\,\bar{\psi}\gamma^\mu D_\mu \psi - \bar{\psi}P_+\left[\varphi, \psi\right] - \bar{\psi}P_-\left[\varphi^\dagger, \psi\right]\Big\}
\end{aligned}
\tag{2.16}
$$

with chiral projection operators $P_\pm = (1 \pm \gamma_5)/2$. When proving this result one may
use that for two Majorana spinors χ_1, χ_2 the trace of $\bar{\chi}_1[\varphi, \chi_2] + \bar{\chi}_2[\varphi, \chi_1]$ vanishes. Un-
der dimensional reduction, the four-dimensional Lorentz transformations in SO$(1,3)$ turn

particle	spin	name
$\overline{\lambda}\gamma_5\lambda$	0	a-η
$\overline{\lambda}\lambda$	0	a-f
$F_{MN}\Sigma^{MN}\lambda$	$\frac{1}{2}$	gluino-glueball

(a) VY multiplet.

particle	spin	name
$F^{MN}F_{MN}$	0	0^{++} glueball
$F^{MN}\epsilon_{MNRS}F^{RS}$	0	0^{-+} glueball
$F_{MN}\Gamma^M D^N\lambda$	$\frac{1}{2}$	gluino-glueball

(b) FGS multiplet.

Table 1. Multiplet structure of $\mathcal{N} = 1$ SYM theory as predicted by low energy effective actions [4, 6].

into two-dimensional Lorentz transformations and flavour rotations for the scalar fields (R-symmetry), i.e.

$$\mathrm{SO}(1,3) \to \mathrm{SO}_L(1,1) \times \mathrm{SO}_R(2), \tag{2.17}$$

and correspondingly $\mathrm{Spin}(1,3)$ turns into $\mathrm{Spin}(1,1)$ and R-transformations of the two spinor fields, generated by $\Sigma_{23} = -\sigma_3 \otimes \mathbb{1}/2$. This R-symmetry acts on the real fields as

$$\begin{pmatrix} \phi_1 \\ \phi_2 \end{pmatrix} \to R(2\alpha) \begin{pmatrix} \phi_1 \\ \phi_2 \end{pmatrix}, \quad \begin{pmatrix} \chi_1 \\ \chi_2 \end{pmatrix} \to R(-\alpha) \begin{pmatrix} \chi_1 \\ \chi_2 \end{pmatrix}, \tag{2.18}$$

where $R(\alpha)$ is a rotation with angle α. The complex fields transform as

$$\varphi \to \exp(2\,\mathrm{i}\,\alpha)\varphi, \quad \psi \to \exp(-\mathrm{i}\,\alpha\,\gamma_5)\psi, \quad \bar{\psi} \to \bar{\psi}\exp(-\mathrm{i}\,\alpha\,\gamma_5), \tag{2.19}$$

which is identified as chiral symmetry in two dimensions. In contrast, the four-dimensional chiral symmetry turns into a phase rotation of the Dirac field,

$$\lambda' = \exp(\mathrm{i}\alpha\,\Gamma_5)\lambda = \begin{pmatrix} \cos\alpha & \gamma_5\sin\alpha \\ -\gamma_5\sin\alpha & \cos\alpha \end{pmatrix} \begin{pmatrix} \lambda_1 \\ \lambda_2 \end{pmatrix} \quad \Rightarrow \quad \psi' = \exp(-\mathrm{i}\,\alpha)\psi \tag{2.20}$$

and implies fermion number conservation in two dimensions. This observation allows us to introduce two different fermion mass terms in the lattice formulation with Wilson fermions. A four-dimensional Majorana mass term proportional to $\bar{\lambda}\lambda$ which violates fermion number conservation in two dimensions or a two-dimensional Dirac mass term $\bar{\psi}\psi$ which violates chiral symmetry. When fine-tuning to the supersymmetric continuum limit we shall break chiral symmetry of the reducible model in order to have the same fermionic symmetries as in the $\mathcal{Q}$-exact formulation in [33], to which we shall compare our results.

2.1 Expected mass spectrum

Veneziano and Yankielowicz were the first to derive a low energy effective Lagrangian for $\mathcal{N} = 1$ SYM theory in four dimensions, in analogy to QCD [4]. They conjectured that the lightest super-multiplet contains the bound states shown in table 1(a): a scalar meson a-f, a pseudoscalar meson a-η and a spin 1/2 bound state between a Majorana fermion and a gauge boson, called gluino-glueball. We refer to this super-multiplet as the VY-multiplet. In a confining theory one also expects glueballs in the particle spectrum. Therefore a second

particle	spin	name
$\overline{\lambda}\Gamma_5\lambda$	0	a-η
$\overline{\lambda}\lambda$	0	a-f
$F_{\mu\nu}\Sigma^{\mu\nu}\lambda + 2\mathrm{i}[\phi_1,\phi_2]\Sigma^{23}\lambda$	$\frac{1}{2}$	gluino-glue/scalarball

particle	spin	name
$[\phi_1,\phi_2]F_{\mu\nu}$	0	glue-scalarball
$F_{\mu\nu}F^{\mu\nu} - 2D_\mu\phi_m D^\mu\phi_m - 2[\phi_1,\phi_2]^2$	0	0^{++}-glueball, scalarball
$F_{\mu\nu}\Gamma^\mu D^\nu\lambda - D_\mu\phi_m\left(\mathrm{i}\Gamma^\mu[\phi^m,\lambda] + \Gamma^{m+1}D^\mu\lambda\right)$ $-[\phi_m,\phi_n]\Gamma^{m+1}[\phi^n,\lambda]$	$\frac{1}{2}$	gluino-glue/scalarball

Table 2. Two-dimensional reduced super-multiplets for the $\mathcal{N} = (2,2)$ theory. In the main body of the text we will call $F_{\mu\nu}\Sigma^{\mu\nu}\lambda$ the gluino-glueball and $[\phi_1,\phi_2]\Sigma^{23}\lambda$ the gluino-scalarball.

super-multiplet was added by Farrar, Gabadadze and Schwetz [6]. The FGS-multiplet is shown in table 1(b). It contains a scalar glueball, a pseudoscalar glueball as well as a spin 1/2 gluino-glueball. Predictions about the mass-hierarchy of the two multiplets vary in the literature [4–7]. In four dimensions large scale Monte-Carlo simulations with Wilson fermions have been performed to investigate the spectrum of bound states [19]. The formation of the VY-multiplet containing both mesons and a gluino-glueball has been observed while the 0^{-+} glueball is significantly heavier. Within (large) errors the 0^{++} glueball has the same mass as the f-meson, but due to mass mixing, it is not clear whether the operator projects onto the correct state. Thus the formation of a heavier multiplet has not been confirmed yet.

The multiplet structure of the $\mathcal{N} = (2,2)$ SYM model can be extracted either from an effective Lagrangian of the two-dimensional system or by dimensionally reducing the super-multiplets of the four-dimensional effective theory. Thereby one should be cautious since the reduced model should contain massless states [26] and a super-multiplet with massless states looks different as a massive super-multiplet. Thus it is not straightforward to foresee the multiplet structure of the reduced system. In any case, the expected bound states — massive or massless — of the $\mathcal{N} = (2,2)$ SYM model are listed in table 2.

2.2 Supersymmetry restoration in the continuum limit

As argued in the introduction, the lattice will break supersymmetry explicitly. To restore it in the continuum limit, we have to fine-tune all relevant supersymmetry breaking operators that are allowed by the remaining symmetries on the lattice. For $\mathcal{N} = (2,2)$ SYM, a discussion of supersymmetry breaking operators is contained in [33]. Thereby the authors use a lattice formulation where one nilpotent supersymmetry is exactly preserved on the lattice. In contrast, in our lattice formulation with Wilson fermions the operator ϕ^2 may show up in the effective action. To cancel this term we must introduce a scalar mass counter-term $m_\mathrm{s}^2\phi^2$ that has to be fine-tuned. The fine-tuned continuum value $m_\mathrm{s}^2 = 0.65948255(8)$

has been calculated to one-loop order (which is sufficient for this theory) in [22]. Although a formulation with compact scalar fields has been used, we checked that this value is also correct for non-compact scalar fields used in our simulation. This can be explained as follows: the Jacobian of the transformation from the compact variables in [22] to non-compact variables cancels (in one-loop) the additional contribution in the action for the compact fields. Thus we find the identical continuum value for $m_{\rm s}^2$ in both formulations.

As for the four-dimensional mother-theory there is only one relevant susy breaking term in two dimensions. Because of the similarity of the two theories one expects an important role of the fermion mass term in two dimensions as well. Let us first recall the impact of a fermion mass in four dimensions. Calculating the Ward identities for the chiral symmetry and the supersymmetry on the lattice, Curci and Veneziano demonstrated that only the renormalized gluino mass will appear as a relevant additional lattice contribution in the Ward identities [8]. Therefore by fine-tuning the bare gluino mass (in our case the fermion mass), one recovers chiral symmetry and supersymmetry in the same limit. We expect the same mechanism to be at work in two dimensions and thus will fine-tune the fermion mass. Note that this idea is in line with [33], as the fermion mass must vanish in the continuum limit to recover the chiral limit, as it is not a relevant operator. A fine-tuning on the lattice will act as an improvement, reducing further supersymmetric violating contributions for finite lattice spacing.

2.3 Euclidean formulation

Since we can not simulate a model with Minkowski spacetime, we must construct a continuation to the corresponding Euclidean theory. This continuation for theories with Majorana fermions was discussed in [56–58]. In contrast to Dirac fermions there is only one Majorana spinor with $\bar{\lambda} = \lambda^{\mathsf{T}} \mathcal{C}$. One cannot impose the reality condition $\bar{\lambda} = \lambda^{\dagger}$. The action picks up an overall negative sign leading to

$$S = \int \mathrm{d}^4 x\, \mathcal{L}, \qquad \mathcal{L} = \mathrm{tr}\left(\frac{1}{4} F_{MN} F^{MN} + \frac{1}{2} \bar{\lambda}\, \Gamma^M D_M \lambda \right) \tag{2.21}$$

with Euclidean Gamma-matrices Γ_M. Majorana fermions exist in the dimensionally reduced Euclidean theory. As convenient representation we may use

$$\Gamma_\mu = \mathbb{1} \otimes \gamma_\mu, \quad \Gamma_2 = \sigma_1 \otimes \gamma_5, \quad \Gamma_3 = \sigma_3 \otimes \gamma_5, \quad \Gamma_5 = -\sigma_2 \otimes \gamma_5, \tag{2.22}$$

now with Euclidean γ_μ. The hermitean matrices $\Gamma_5 = \Gamma_0 \Gamma_1 \Gamma_2 \Gamma_3$ and $\gamma_5 = \mathrm{i}\gamma_0\gamma_1$ are related as $\Gamma_5 = -\sigma_2 \otimes \gamma_5$. Rescaling the fields and absorbing the volume of the torus in a dimensionful gauge coupling the Lagrangian of the reduced Euclidean model reduces to

$$\mathcal{L} = \frac{1}{2g^2}\, \mathrm{tr}\left\{ \frac{1}{2} F_{\mu\nu}^2 + \left(D_\mu \phi_m \right)^2 - \frac{1}{2}\left[\phi_m, \phi_n \right]^2 + \bar{\lambda}\Gamma^\mu D_\mu \lambda - \mathrm{i}\bar{\lambda}\, \Gamma^{m+1}\left[\phi_m, \lambda \right] \right\}. \tag{2.23}$$

In terms of complex fields ψ and φ it takes the form

$$\begin{aligned} \mathcal{L} = \frac{1}{g^2}\, \mathrm{tr}\Big\{ & \frac{1}{4} F_{\mu\nu}^2 + \frac{1}{2}(D_\mu \varphi)^\dagger (D^\mu \varphi) + \frac{1}{8}\left[\varphi^\dagger, \varphi \right]^2 \\ & + \bar{\psi}\gamma^\mu D_\mu \psi + \mathrm{i}\,\bar{\psi} P_+[\varphi, \psi] + \mathrm{i}\,\bar{\psi} P_-[\varphi^\dagger, \psi] \Big\}. \end{aligned} \tag{2.24}$$

In actual simulations we choose the formulation (2.23) with two real scalar fields and a reducible four-component Majorana spinor.

2.4 Ward identities

In order to check for the restoration of supersymmetry in the continuum limit, we monitor supersymmetric Ward identities

$$\langle \mathcal{Q}\mathcal{O} \rangle = 0, \tag{2.25}$$

with supercharge $\mathcal{Q}$ introduced in (2.4) and operators $\mathcal{O}$. In four dimensions the fermionic operator

$$\mathcal{O}_a(x) = \mathrm{tr}_\mathrm{c} \left\{ \overline{\lambda}_b(x) \big(\Gamma^{MN}\big)^b{}_a F_{MN}(x) \right\} \tag{2.26}$$

is frequently used and gives rise to a bosonic Ward identity [48]. On a finite lattice with lattice constant a supersymmetry is violated and in terms of the rescaled dimensionless lattice fields the approximate Ward identity reads

$$\begin{aligned} \frac{1}{N_t N_s} \langle S_\mathrm{B} \rangle = \langle \mathcal{L}_\mathrm{B} \rangle = \frac{1}{4} \big\langle \mathrm{tr}\, F^{MN} F_{MN} \big\rangle &= -\frac{3}{8}\frac{1}{2} \big\langle \mathrm{tr}\, \overline{\lambda} \slashed{D} \lambda \big\rangle + O\big(\beta^{-1}\big) \\ &= \frac{3}{2}\big(N_c^2 - 1\big) + O\big(\beta^{-1}\big) = \frac{9}{2} + O\big(\beta^{-1}\big), \quad \frac{1}{\beta} = (ag)^2. \end{aligned} \tag{2.27}$$

We made use of the fact that by translational invariance expectation values of densities do not depend on the site x. The identity relates the expectation values of the bosonic and fermionic parts of the action, up to a one-loop term of order $1/\beta$ which originates from the violation of supersymmetry. Note that in the on-shell formulation, one obtains the factor of $\frac{3}{8}$ instead of the factor $\frac{1}{2}$ in the off-shell formulation [48].

In accordance with the dimensional reduction we decompose the operator (2.26) into three terms: one with $\{M,N\}$ being $\{m,n\}$, one with $\{\mu,\nu\}$ and finally one with $\{m,\mu\}$ or $\{\mu,m\}$. The corresponding three (two-dimensional) Ward identities read

$$\begin{aligned} W_1 &= \frac{1}{2}\big\langle\, [\phi_1,\phi_2]^2 \,\big\rangle - \frac{\mathrm{i}}{8}\big\langle \overline{\lambda}\Gamma_2\,[\phi_1,\lambda] + \overline{\lambda}\Gamma_3\,[\phi_2,\lambda] \,\big\rangle = 0\,, \\ W_2 &= \frac{1}{4}\big\langle F_{\mu\nu} F^{\mu\nu} \big\rangle + \frac{\mathrm{i}}{8}\big\langle \overline{\lambda}\,\Gamma_2\,[\phi_1,\lambda] - \overline{\lambda}\,\Gamma_3\,[\phi_2,\lambda] \,\big\rangle = \frac{3}{2}, \\ W_3 &= \frac{1}{2}\big\langle D_\mu \phi^m D^\mu \phi_m \big\rangle = 3. \end{aligned} \tag{2.28}$$

Note that the sum rule $W_1 + W_2 + W_3$ just reproduces the result $\frac{9}{2}$ in (2.27).

3 Lattice formulation

In the simulations we use Wilson fermions and the tree-level improved Lüscher-Weisz gauge action [59]. The scalar fields are treated as non-compact site-variables in the adjoint representation of the gauge group. The action for the scalar fields is implemented by using the forward difference

$$D_\mu^\mathrm{f} \phi_x = \phi_{x+e_\mu} - U_{x,\mu}^\mathrm{A} \phi_x \tag{3.1}$$

in the kinetic term, where the link variables $U_{x,\mu}^{\mathrm{A}}$ are in the adjoint representation. The fermion operator for Wilson fermions is

$$D_{xy} = (m_{\mathrm{f}} + 2 + \Gamma_{m+1} f^a \phi_a^m)\, \delta_{x,y} - \frac{1}{2} \sum_\mu \left(\mathbb{1} - \Gamma_\mu\right) \delta_{x+e_\mu,y} U_{x,\mu}^{\mathrm{A}} + \left(\mathbb{1} + \Gamma_\mu\right) \delta_{x-e_\mu,y} U_{y,\mu}^{\mathrm{A}}{}^{\mathsf{T}}$$

$$(3.2)$$

where the matrices $(f^a)_{bc}$ are the structure constants of the gauge group SU(2). Integration over the Majorana fermion yields the Pfaffian of $\mathcal{C}D$ and we obtain for the partition function as integral over the bosonic fields,

$$Z = \int \mathcal{D}U \mathcal{D}\phi \; \mathrm{Sign}(\mathrm{Pf}(\mathcal{C}D)) \; \det(D^\dagger D)^{\frac{1}{4}} \, e^{-S[U,\phi]}. \tag{3.3}$$

We made use of the Γ_5-hermiticity of the fermion operator $\Gamma_5 D \Gamma_5 = D^\dagger$. The fourth root of $D^\dagger D$ is approximated by a rational approximation in the rHMC [60–63] algorithm.

3.1 Sign problem and flat directions

Two known problems may potentially spoil the Monte-Carlo simulations: a potential sign problem introduced by the Pfaffian and possible *flat directions* in which the scalar potential is constant. We address both issues in turn. Although the eigenvalues λ_i of the hermitian matrix $Q = \Gamma_5 D$ are real and doubly degenerate [12], the Pfaffian can still introduce a sign problem that we have to take into account in the simulations. Using the dependence of the Pfaffian on the hopping parameter $\kappa = 1/(2\,m_{\mathrm{f}} + 4)$ it is possible to show [15] that the Pfaffian and the determinant are related by

$$\det D = \prod_i \lambda_i^2 \quad \Rightarrow \quad \mathrm{Pf}(\mathcal{C}D[U]) = \prod_i \lambda_i \,. \tag{3.4}$$

We use the nice spectral flow method introduced in [15] to monitor a potential sign problem. The idea is that for a given gauge field configuration (a typical one for fixed β and κ) the eigenvalues λ_i vary continuously when the hopping parameter κ_{spec} in the fermion operator increases. For the free operator with $\kappa_{\mathrm{spec}} = 0$ the Pfaffian is positive. Therefore, the Pfaffian can only become negative if an odd number of eigenvalues $\lambda_i(\kappa_{\mathrm{spec}})$ change their signs as a function of κ_{spec}. We have monitored the 8 eigenvalues with smallest absolute values, shown in the left panel of figure 1 for configurations generated with $\beta = 15.5$ and $\kappa = 0.27020$ as function of the flow parameter κ_{spec} increasing from 0 to the value of interest κ. The positive eigenvalues decrease monotonously while the negative eigenvalues increase as $\kappa_{\mathrm{spec}} \to \kappa$, but they do not cross zero such that the Pfaffian for this configuration remains positive. Furthermore we show the smallest eigenvalues for three ensembles of 1000 gauge configurations each belonging to the three flow parameters $\kappa_{\mathrm{spec}} = \kappa$, 0.25379, 0.26174 in figure 1. Even for $\kappa_{\mathrm{spec}} = \kappa$ no eigenvalue is small enough to change its sign. Hence the sign of the Pfaffian is always positive. We repeated the simulation for different volumes, inverse gauge couplings and hopping parameters. For $\kappa < \kappa_{\mathrm{c}}$ we never observed a negative Pfaffian while for $\kappa > \kappa_{\mathrm{c}}$ approximately one in thousand configurations had a negative sign. Thus we safely conclude that there is no sign problem in our simulations.

The scalar potential
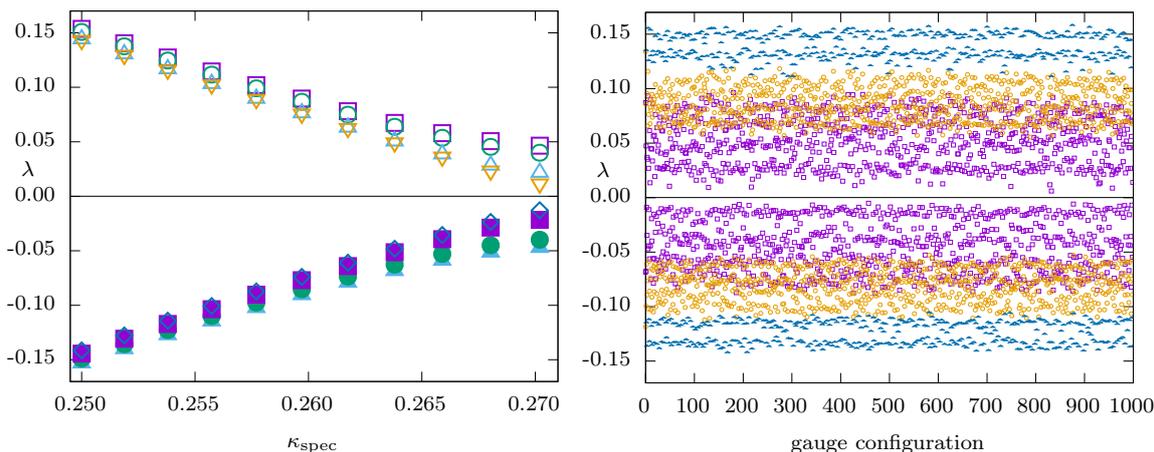
$$V[\phi_1, \phi_2] = [\phi_1, \phi_2]^2 \tag{3.5}$$

Figure 1. Left: spectral flow of 8 eigenvalues with smallest absolute values for $\beta = 15.5$, $\kappa = 0.27020$ on a 64×32 lattice. Right: smallest eigenvalues for three different values of the spectral flow parameter κ_{spec}: 0.25379 (blue triangles), 0.26174 (orange circles) and κ (purple squares).

in the bosonic action is invariant under a shift

$$\phi_1 \to \phi_1 + \alpha \, \phi_2 \qquad \phi_2 \to \phi_2 \,, \tag{3.6}$$

where α is an arbitrary real parameter. This is an example of a *flat direction* in the space of fields (ϕ_1, ϕ_2) along which the potential is constant. Flat directions are generic for SYM theories with extended susy and may destabilize Monte-Carlo simulations since the scalar fields may escape along these directions. Flat directions may either be lifted dynamically by quantum corrections or explicitly by introducing a mass term $m_{\mathrm{s}}^2 \phi^2$. Actually, as emphasized earlier, on the lattice we *must* introduce a mass term with finite m_{s} to find the correct supersymmetric continuum limit. This term (which is needed even for $a \to 0$) lifts the flat directions explicitly. This is shown in figure 2 where we plotted the spatial average $\overline{\phi^2} = \frac{1}{V} \sum \phi_x^2$ as function of Monte-Carlo time for $\beta = 14$, $\kappa = 0.27233$ on a 64×32 lattice in the left panel and the expectation value of $\overline{\phi^2}$ as function of m_{s} in the right panel. For all sets of parameters considered, the absolute value of the scalar fields does not run away. Hence we conclude, that flat directions are lifted for values m_{s} near the value of the supersymmetric model and thus cause no problems in the simulations. In a previous work the lifting of flat directions has been observed even for the susy-breaking value $m_{\mathrm{s}}^2 = 0$ and small values of the inverse gauge coupling [64].

3.2 Scalar and fermion mass fine tuning

The scalar mass is the only relevant coupling that has to be fine-tuned to restore supersymmetry in the continuum limit (in two dimensions the fermion mass needs not be fine-tuned). Its value in the thermodynamic and continuum limit is analytically known from one-loop perturbation theory $m_{\mathrm{s}}^2 = 0.65948255(8)$ [22]. On the finite 64×32 lattice the mass is shifted towards the smaller value $m_{\mathrm{s}}^2 = 0.62849$. In order to investigate the dependence of expectation values on m_{s}^2 we performed simulations for a larger range $m_{\mathrm{s}}^2 \in [0,1]$. Although
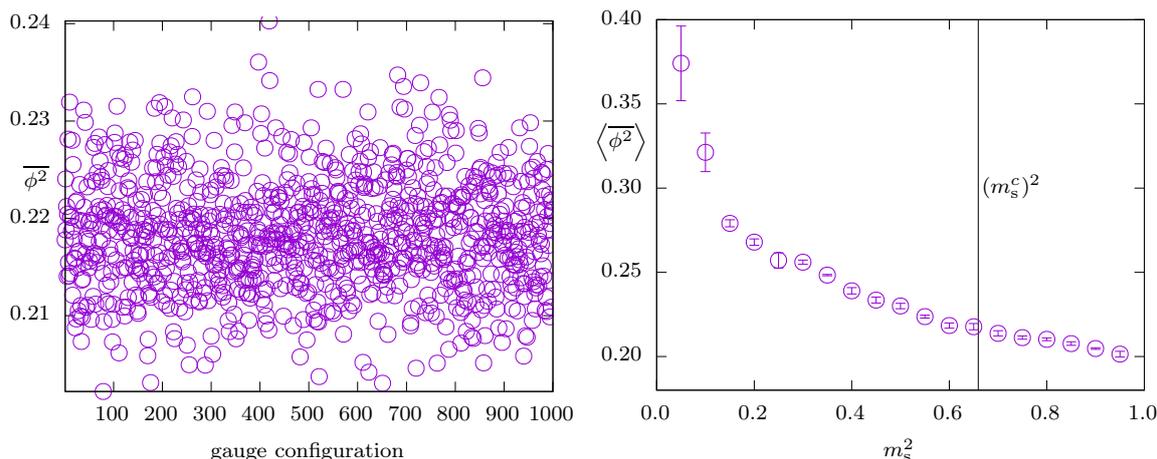
Figure 2. Spatial average of squared scalar field as function of Monte-Carlo time for $\beta = 14$, $\kappa = 0.27233$, $m_s^2 = 0.6594826$ (left) and its expectation as function of m_s^2 (right) on a 16×16 lattice.

the scalar mass breaks supersymmetry explicitly, it turns out that within the statistical uncertainties the Ward identities are independent of the scalar mass. Therefore we set the scalar mass to the continuum value $m_s^2 = 0.6594826$.

In contrast to four-dimensional $\mathcal{N} = 1$ SYM theory, a fine-tuning of the bare fermion mass m_f is not necessary to restore supersymmetry in the continuum limit. Nevertheless we shall enhance the chiral properties on the lattice by tuning m_f to its critical value $m_f^c(L, \beta)$, that depends on the inverse gauge coupling β but depends little on the lattice size. In the continuum limit, the critical fermion mass should approach $m_f^c = 0$, in agreement with the results in [22, 33]. There are two straightforward methods to determine the critical fermion mass on a finite lattice. The first uses the order parameter for chiral symmetry $\langle \bar{\lambda}\lambda \rangle$ and defines m_f^c by the peak position of the chiral susceptibility. The second method comes from an analogy to QCD which is also employed in the four-dimensional $\mathcal{N} = 1$ SYM theory [4, 16, 65]: although the pion is not a physical particle in the theory, one can define its correlation function in a partially quenched setup (for details see also appendix B) which mimics a second Majorana flavour in $\mathcal{N} = 1$ SYM. The pion mass is related to the renormalized gluino mass by

$$m_q \propto m_\pi^2. \tag{3.7}$$

We expect this relation to hold in two dimensions as well and define the critical fermion mass at the value where the gluino mass vanishes. The results for the two methods are given in table 3. Both methods yield comparable values for the critical fermion mass. One observes that the fermion mass approaches the expected continuum value from below.

In the following section we show that $\sqrt{\beta} \propto a$. Therefore we extrapolate our results to the continuum with the ansatz

$$m_f^c(\beta) = m_\infty + c_1 \beta^{-e_1} + c_2 \beta^{-e_2} . \tag{3.8}$$

The coefficients c_i encode lattice artifacts and in the continuum limit $m_f^c(\beta \to \infty) = m_\infty$.

β	14.0	15.5	17.0	40
$m_{\mathrm{f}}^{\mathrm{c}}(\chi_s)$	$-0.1738(8)$	$-0.1595(7)$	$-0.1488(4)$	$-0.0757(4)$
$m_{\mathrm{f}}^{\mathrm{c}}(\pi)$	$-0.1730(11)$	$-0.1615(6)$	$-0.1511(7)$	$-0.0756(7)$
β	60	80	100	
$m_{\mathrm{f}}^{\mathrm{c}}(\chi_s)$	$-0.0553(3)$	$-0.0448(3)$	$-0.0380(5)$	
$m_{\mathrm{f}}^{\mathrm{c}}(\pi)$	$-0.0542(4)$	$-0.0433(26)$	$-0.0365(6)$	

Table 3. Critical fermion mass $m_{\mathrm{f}}^{\mathrm{c}}$ for different β. To determine the mass we use the chiral susceptibility and the mass of the pion ground state.

m_∞	c_1	c_2	e_1	e_2	χ_{w}^2	χ^2
$0.0051(26)$	$-0.285(32)$	$-1.44(8)$	$\underline{1/2}$	$\underline{1}$	1.33	6.33×10^{-7}
$-0.0126(8)$	$-2.64(5)$	$5.48(69)$	$\underline{1}$	$\underline{2}$	2.31	7.88×10^{-7}
$-0.0041(18)$	$-1.48(6)$	$\underline{0}$	$0.820(18)$	$-$	1.06	5.42×10^{-7}

Table 4. Fit values for the fit function given in (3.8), for three different sets of parameters. The mass m_∞ represents the continuum value of the critical fermion mass $m_{\mathrm{f}}^{\mathrm{c}}$, which should be zero. The underlined parameters are prescribed in the 2-parameter fits.

Since $m_{\mathrm{f}}^{\mathrm{c}}(\beta)$ does not depend significantly on the lattice size, we also include simulations at $\beta = 40, 60, 80, 100$ on smaller lattices into the extrapolation. The results of the fits are shown in table 4. We give two different values χ_{w}^2 and χ^2 for the goodness of the fit. The first χ_{w}^2 was calculated including the errors for $m_{\mathrm{f}}^{\mathrm{c}}$ as weights in the fit and the second χ^2 without weights. χ^2 is much smaller, showing that the fit of the given ansatz to the data is very good, but the errors for the critical masses are probably underestimated.[1] Within uncertainties the values for m_∞ are compatible with the expected result $m_\infty = 0$.

3.3 Wilson loops and confinement

In order to determine the lattice spacing and perform the continuum limit in section 3.4, we consider the static quark-antiquark potential

$$V(r) = A + \sigma r \tag{3.9}$$

in the fundamental representation of SU(2) with the string tension σ. In two dimensions the Coulomb potential is a linear function in r and the Lüscher term is absent. Hence we do not expect a $1/r$ term for small and large separations of the static charges. For large separations of the charges the potential may flatten if there is string breaking. If there is screening by massless particles then the string tension should vanish.

In this subsection we calculate the static quark-antiquark potential to see whether the theory is confining or whether the fermions can screen the external charges. In addition to the theory of investigation we calculate the potential for the simpler $\mathcal{N} = (1, 1)$ SYM

---

[1]The errors given for the critical fermion masses $m_{\mathrm{f}}^{\mathrm{c}}$ include only fit errors but not statistical errors.

theory in two dimensions. The latter is obtained by a dimensional reduction of the three-dimensional $\mathcal{N} = 1$ SYM theory and its action in the continuum reads

$$S = \frac{1}{2g^2} \int \mathrm{d}^2x \, \mathrm{tr} \left\{ -\frac{1}{2} F_{\mu\nu} F^{\mu\nu} + \mathrm{i}\bar{\lambda}\gamma^\mu D_\mu \lambda + D_\mu \phi D^\mu \phi - \mathrm{i}\bar{\lambda}\gamma_5 [\phi, \lambda] \right\} . \tag{3.10}$$

It contains one adjoint scalar ϕ as well as one adjoint Majorana fermion λ. The γ^μ are two-dimensional matrices as they are for the three-dimensional mother theory. It has been argued in [66, 67] that in $\mathcal{N} = (1, 1)$ SYM theory a cloud of massless gluinos screens a static quark in the fundamental representation. When the gluinos become massive, supersymmetry is broken, screening disappears and confinement should be observed. It is believed that this is a generic feature of two-dimensional YM-theories with massless adjoint fermions.

Our lattice results for the static quark-antiquark potential $V_T(R) = \log\left(\frac{W_{R,T}}{W_{R,T+1}}\right)$ with Wilson loops $W_{R,T}$ are shown in figure 3. For both theories[2] we find a linear raising potential. To suppress statistical fluctuations, we used different numbers of STOUT smearing steps. With more smearing the potential becomes flatter, since fluctuations on scales of the final broken-string state are suppressed. We also measured Wilson-loops with unusual small T to amplify the signal to noise ratio. For $T \approx R > 10$ the errors become large since the signals are exponentially suppressed. The unsmeared and smeared data (with controlled statistical errors) both show no evidence of string breaking. If there would be screening for massless fermions, then the string tension should tend to zero for light fermions. We performed simulations for several values of the fermion mass $m_\mathrm{f} \in [-0.1640, 0.0]$ and always obtained a linear rising potential. The string tension decreases approximately 10% towards the chiral limit. Hence there seems to be no signal of screening in the simulations. It may be that the Wilson loop has a poor overlap to the broken-string ground state, but this seems unlikely since its behavior does not change even close to the chiral limit. Another explanation could be, that in a compact formulation of gauge theories certain states are projected out of the Hilbert space and screening cannot occur. Of course, for an affirmative answer we would need a larger set of operators and higher statistics or even better, a method similar to the multi-level Lüscher-Weisz algorithm with exponential error reduction, as it exists for pure gauge theories [68, 69].

3.4 Scale setting and lattice spacing

In order to determine the lattice spacing and perform the continuum limit, we consider the static quark-antiquark potential in the fundamental representation of SU(2) and extrapolate with the expected form (3.9) to the chiral limit. For $\beta = 17$ and $\kappa = 0.26655$ the potential is shown in figure 4. To compare our results to usual QCD lattice data, we employ the Sommer scale [70] and define a lattice spacing in physical units. The results for three different values of the inverse gauge coupling

$$\beta = \frac{1}{a^2 g^2} \tag{3.11}$$

---

[2]The $\mathcal{N} = (1, 1)$ SYM theory suffers from a mild sign problem which can be treated with the help of a exact reweighing by measuring the Pfaffian.
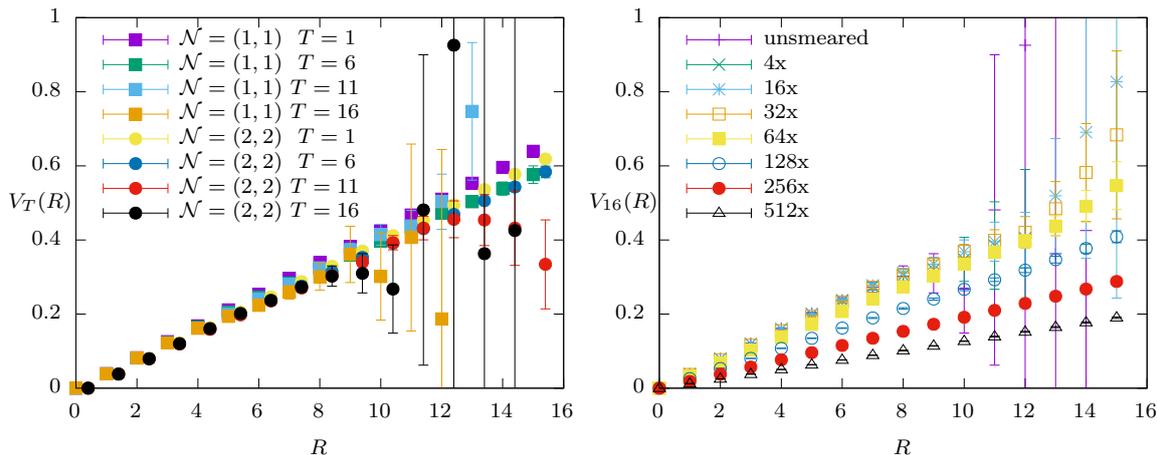
Figure 3. Left: static fundamental quark-antiquark potential of $\mathcal{N} = (1,1)$ and $\mathcal{N} = (2,2)$ SYM theory. The measurements where done for several temporal extends T on the 64×32 lattice including reweighting of the Pfaffian. The $\mathcal{N} = (2,2)$ data is shifted slightly for clarity of presentation. Right: comparison of different levels of STOUT smearing with smearing parameter $\epsilon = 0.4$ for the $\mathcal{N} = (2,2)$ SYM with temporal Wilson loop size $T = 16$.
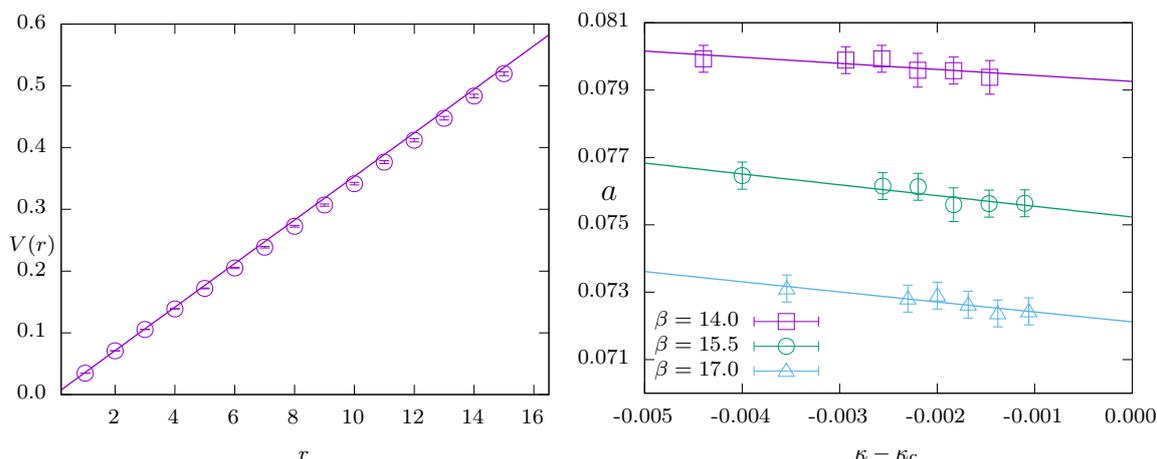

Figure 4. Left: static quark potential and fit to (3.9) for $\beta = 17.0$ and $\kappa = 0.26655$. Right: lattice spacing a for $\beta = 14.0$, 15.5 and 17.0 as function of κ on a 64×32 lattice.

are depicted in table 5. Since the lattice spacing a depends on the fermion mass, we extrapolate the latter to its chiral limit $m_{\mathrm{f}} = m_{\mathrm{f}}^{\mathrm{c}}$. The results are given in table 5. In the last rows we checked that the inverse dimensional coupling $1/g^2 = \beta a^2$ in (3.11) is almost independent of β, confirming that the continuum limit is reached for $\beta \to \infty$.

3.5 Smearing

We use three different types of smearing. For the scalar fields we utilize the low pass filter for functions. This smearing process is defined as

$$\tilde{\phi}^n(x) = (1 + \epsilon \Delta) \, \tilde{\phi}^{n-1}(x) \quad \text{with} \quad \tilde{\phi}^0(x) = \phi(x), \tag{3.12}$$

$\beta = 14.0$			$\beta = 15.5$		
$\kappa - \kappa_{\mathrm{c}}$	$a[\mathrm{fm}]$	$\beta a^2[\mathrm{fm}]$	$\kappa - \kappa_{\mathrm{c}}$	$a[\mathrm{fm}]$	$\beta a^2[\mathrm{fm}]$
-0.00440	$0.07993(4)$	$0.08944(9)$	-0.00400	$0.07646(4)$	$0.09062(9)$
-0.00294	$0.07989(4)$	$0.08935(9)$	-0.00256	$0.07612(4)$	$0.08981(9)$
-0.00257	$0.07993(4)$	$0.08944(9)$	-0.00220	$0.07613(4)$	$0.08983(9)$
-0.00220	$0.07959(5)$	$0.08838(11)$	-0.00183	$0.07560(5)$	$0.08859(12)$
-0.00183	$0.07958(4)$	$0.08833(9)$	-0.00167	$0.07563(4)$	$0.08866(9)$
-0.00146	$0.07938(5)$	$0.08822(11)$	-0.00110	$0.07564(4)$	$0.08868(9)$
0	$0.07926(322)$	$0.08795(51)$	0	$0.07524(310)$	$0.08774(47)$
$\beta = 17.0$					
$\kappa - \kappa_{\mathrm{c}}$	$a[\mathrm{fm}]$	$\beta a^2[\mathrm{fm}]$	$\kappa - \kappa_{\mathrm{c}}$	$a[\mathrm{fm}]$	$\beta a^2[\mathrm{fm}]$
-0.00354	$0.07311(4)$	$0.09087(10)$	-0.00168	$0.07263(4)$	$0.08968(10)$
-0.00230	$0.07281(4)$	$0.09012(10)$	-0.00138	$0.07237(4)$	$0.08904(10)$
-0.00200	$0.07290(4)$	$0.09034(10)$	-0.00106	$0.07243(4)$	$0.08918(10)$
0	$0.07212(266)$	$0.08842(38)$			

Table 5. Lattice spacing for different combinations of β and m_{f}. In the last rows of each β section we give the extrapolations to the chiral limit.

where $\phi(x)$ is the scalar field, $\tilde{\phi}^n(x)$ is the smeared field and ϵ is the smearing parameter. For gauge fields we use STOUT smearing [71] and for the fermionic sinks and sources we apply Jacobi smearing [72, 73]. In table 6 we give the number of configurations generated for the given sets of parameters $\{\beta, m_{\mathrm{f}}, m_{\mathrm{s}}\}$ on a 64×32 lattice. A large number of configurations is needed to extract the masses of the ground- and excited states of the f-meson. This is due to large fluctuations of the two scalar fields entering the fermion operator via the Yukawa terms which give rise to strong fluctuations in the fermion correlators.

4 Restoration of Ward identities

The simple continuum Ward identities (2.28) do not hold on the lattice since (in our formulation) there are just no supersymmetries which leave the lattice action invariant. But in the continuum limit we must recover these identities if we take the finite additive renormalization of the parameter m_{s}^2 into account.

Inspired by the treatment of four-dimensional models in [8, 14, 74–76] we impose three rules to define the lattice transformations:

1. They become the continuum susy transformations in the continuum limit.
2. They commute with the gauge transformations.
3. The transformation of the covariant derivative is the lattice equivalent of the continuum counterpart.

β	m_{f}	m_{s}^2	# C		β	m_{f}	m_{s}^2	# C
14.0	-0.1440	0.6594826	10000		15.5	-0.1470	0.6594826	10000
14.0	-0.1550	0.6594826	10000		15.5	-0.1495	0.6594826	10000
14.0	-0.1565	0.6594826	10000		15.5	-0.1520	0.6594826	10000
14.0	-0.1590	0.6594826	10000		17.0	-0.1242	0.6594826	10000
14.0	-0.1615	0.6594826	10000		17.0	-0.1329	0.6594826	10000
14.0	-0.1640	0.6594826	10000		17.0	-0.1350	0.6594826	10000
15.5	-0.1320	0.6594826	10000		17.0	-0.1372	0.6594826	10000
15.5	-0.1420	0.6594826	10000		17.0	-0.1393	0.6594826	10000
15.5	-0.1445	0.6594826	10000		17.0	-0.1415	0.6594826	10000

Table 6. Number of Configurations (# C) for the given parameters β, m_{f} and m_{s} on a 64×32 lattice.

These rules allow us to reduce the plethora of possible lattice transformations acting on the lattice fields $\{U_\mu(x), \lambda(x), \phi_m(x)\}$ to a small set. We choose the transformations

$$\bar{\mathcal{Q}}^\alpha U_\mu(x) = \frac{a}{2} U_\mu(x)(\Gamma_\mu)^\alpha{}_\beta \lambda^\beta(x + ae_\mu), \quad \bar{\mathcal{Q}}^\alpha U_\mu^\dagger(x) = -\frac{a}{2}(\Gamma_\mu)^\alpha{}_\beta \lambda^\beta(x + ae_\mu)U_\mu^\dagger(x),$$

$$\bar{\mathcal{Q}}^\alpha \lambda_\beta = 0, \quad \bar{\mathcal{Q}}^\alpha \bar{\lambda}_\beta = -(\Gamma_{\mu\nu})^\alpha{}_\beta G^{\mu\nu}, \quad \bar{\mathcal{Q}}^\alpha \phi_m = \frac{1}{2}(\Gamma_{m+1})^\alpha{}_\beta \lambda^\beta, \tag{4.1}$$

where all fields but U_μ carry the canonical dimensions in four dimensions and $a^2 G^{\mu\nu}$ is the clover plaquette. Since the lattice action is not invariant the continuum Ward identities are deformed to lattice identities

$$\langle \bar{Q}O \rangle = \langle O \, \bar{Q}S_{\text{lat}} \rangle, \tag{4.2}$$

where the transformation of the Lagrangian is given by

$$\bar{Q}^\alpha \mathcal{L}_{\text{lat}} = \frac{\beta}{2} \left\{ \partial_\mu s_\mu^\alpha - (m_{\text{f}} - m_{\text{f}}^{\text{c}}) \, \chi_{\text{f}}^\alpha + \left(m_{\text{s}}^2 - (m_{\text{s}}^{\text{c}})^2 \right) \chi_{\text{s}}^\alpha \right\} + \mathcal{O}(a) \tag{4.3}$$

with dimensional quantities $\mathcal{L}_{\text{lat}}$ and β. After summing over all lattice sites the contribution of the supercurrent s_μ^α vanishes, up to terms of order $\mathcal{O}(a)$. In addition, the terms χ_{f}^α and χ_{s}^α represent corrections introduced by a nonzero fermion mass m_{f} and scalar mass m_{s} away from their critical values. These terms are suppressed after fine-tuning the masses. Details of the calculation are given in appendix A. Finally we obtain the lattice Ward identities in the chiral limit $m_{\text{f}} \to m_{\text{f}}^{\text{c}}$

$$W_{\text{B}} = \beta V^{-1} \langle S_{\text{B}} \rangle + m_{\text{s}}^2 \langle \operatorname{tr} \phi^2 \rangle \to \frac{9}{2}, \quad W_3 = \frac{\beta}{2} \langle \operatorname{tr} D_\mu \phi^a D^\mu \phi_a \rangle + m_{\text{s}}^2 \langle \operatorname{tr} \phi^2 \rangle \to 3,$$

$$W_2 = \frac{\beta}{4} \langle \operatorname{tr} F_{\mu\nu} F^{\mu\nu} \rangle + \beta \langle \operatorname{tr} \bar{\lambda}\Upsilon \rangle \to \frac{3}{2}, \quad W_1 = \frac{\beta}{2} \langle \operatorname{tr} [\phi_1, \phi_2]^2 \rangle - \beta \langle \operatorname{tr} \bar{\lambda} \Upsilon \rangle \to 0, \tag{4.4}$$

where we used the abbreviation

$$\Upsilon = \frac{\text{i}}{8} \big(\Gamma_2 [\phi_1, \lambda] + \Gamma_3 [\phi_2, \lambda] \big). \tag{4.5}$$
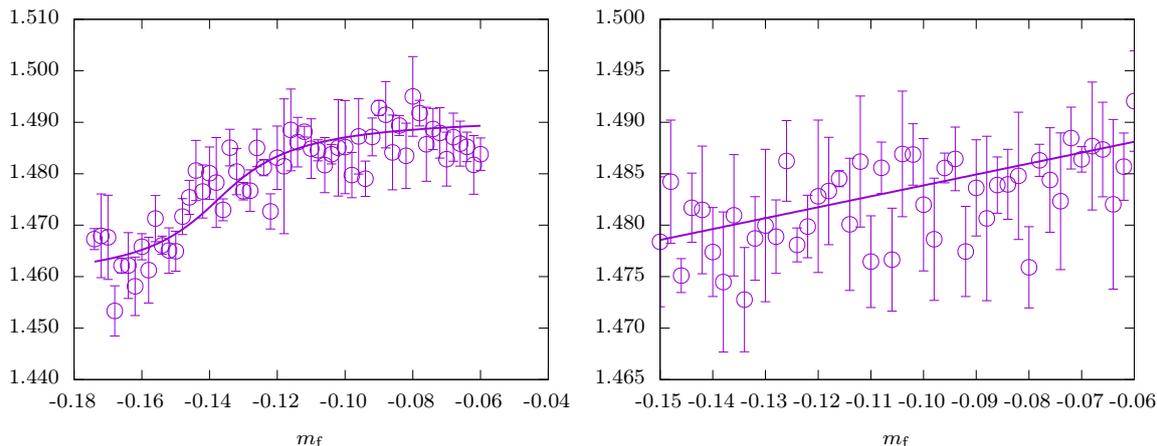
– 18 –

Figure 5. The Ward identity W_2 in (4.4) is shown for $\beta = 17$ (left) and $\beta = 40$ (right).

4.1 Extrapolation to the chiral limit

We did check that the Ward identities show no dependence on the lattice size for $L_{S,T} > 8$ for all β. Thus we simulated on a moderate 32×16 lattice with parameters $\beta = 40, 60, 80, 100$. To extrapolate our results to the chiral limit we need a guess for the functional dependence of the Ward identities on the bare mass m_f. In two dimensions there is no spontaneous symmetry breaking and correlators are smooth functions of m_f. Our simulations indicate that bosonic correlators show, up to an additive constant b, a smoothed step function behavior on the fermion mass. This motivates the following ansatz for their m_f-dependence near the *critical* fermion bare mass m_*:

$$W(m_f) \sim a \arctan\{\xi(m_f - m_*)\} + b \qquad (4.6)$$

with fit parameters a, b, m_* and ξ, where ξ is to be interpreted as lattice correlation length.

For example, in the left panel of figure 5 we depicted the arctan-fit to the Ward identity W_2 which is dominated by the term quadratic in the field strength tensor. We observe that our ansatz yields a good approximation for the functional dependence of the data on m_f. The extracted value for m_* is very close to the critical fermion mass m_f^c. For $\beta \gtrsim 40$ this ansatz is not appropriate anymore and we use a linear fit function, as seen on the right hand side of figure 5. These fits allow us to study the Ward identities in the chiral limit.

Finally we have to extrapolate the Ward identities to the continuum limit. In figure 6 we show the results for W_1 and the two contributions to W_2 in (4.4) for different β. In all cases we observe a monotonic convergence with increasing β.

In table 7 we listed the values of all Ward identities for the chiral limit and different β together with the expected continuum value. The plots in figure 7 show the dependence on β. The Ward identities clearly converge to the supersymmetric continuum value. In order to extrapolate to the continuum limit, we use three different fits of the form

$$W(\beta) = W^\infty + b\,\beta^{-c} \qquad (4.7)$$

with the prescribed value $c = 1/2$ for Fit 1 and $c = 1$ for Fit 2 (b and W^∞ are free fit parameters). Fit 3 has three free fit parameters. The fits are shown in figure 7. In table 7
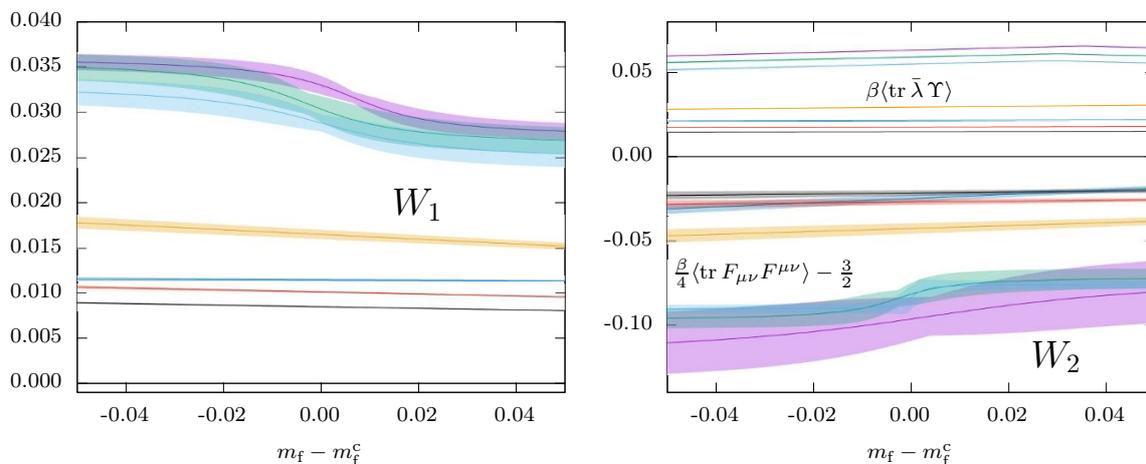
Figure 6. Ward identities (4.4) as functions of $m_\mathrm{f} - m_\mathrm{f}^\mathrm{c}$ for various values of β between 14 and 100. The colors represent different β: 14 •, 15.5 •, 17 •, 40 •, 60 •, 80 • and 100 •. For W_1 (left panel) we show the fits and standard deviations (confident band). For W_2 (right panel) we show the two components $\beta\langle \mathrm{tr}\,\bar{\lambda}\Upsilon \rangle$ (upper half) and $\frac{\beta}{4}\langle \mathrm{tr}\,F_{\mu\nu}F^{\mu\nu}\rangle$ (lower half).

Ward identity	W_1	W_2	W_3	W_B
$\beta = 14.0$	0.0323(8)	1.4678(79)	3.0222(5)	4.5241(126)
$\beta = 15.5$	0.0304(16)	1.4732(118)	3.0231(8)	4.5298(143)
$\beta = 17.0$	0.0288(10)	1.4688(38)	3.0185(9)	4.5197(128)
$\beta = 40.0$	0.0165(5)	1.4834(6)	3.0007(6)	4.4867(11)
$\beta = 60.0$	0.0123(1)	1.4918(6)	2.9968(8)	4.5053(6)
$\beta = 80.0$	0.0101(1)	1.4901(6)	2.9977(6)	4.4973(9)
$\beta = 100.0$	0.0085(1)	1.4920(5)	2.9972(6)	4.5004(8)
$\beta \to \infty$ (Fit 1)	$-0.0053(3)$	1.5105(71)	2.9773(66)	4.4825(140)
$\beta \to \infty$ (Fit 2)	0.0046(1)	1.4981(46)	2.9909(27)	4.4936(74)
$\beta \to \infty$ (Fit 3)	$-0.0021(14)$	1.5507(872)	3.0006(125)	4.5492(1011)
$\beta \to \infty$ (weighted average)	$-0.0024(13)$	1.5267(424)	2.9885(70)	4.5128(507)
theor. value	0	$\frac{3}{2}$	3	$\frac{9}{2}$

Table 7. Values of Ward identities for different values of β on a 32×16 lattice. The last five rows contain the continuum extrapolations with three different fit functions and a weighted average as well as the theoretical value for unbroken susy.
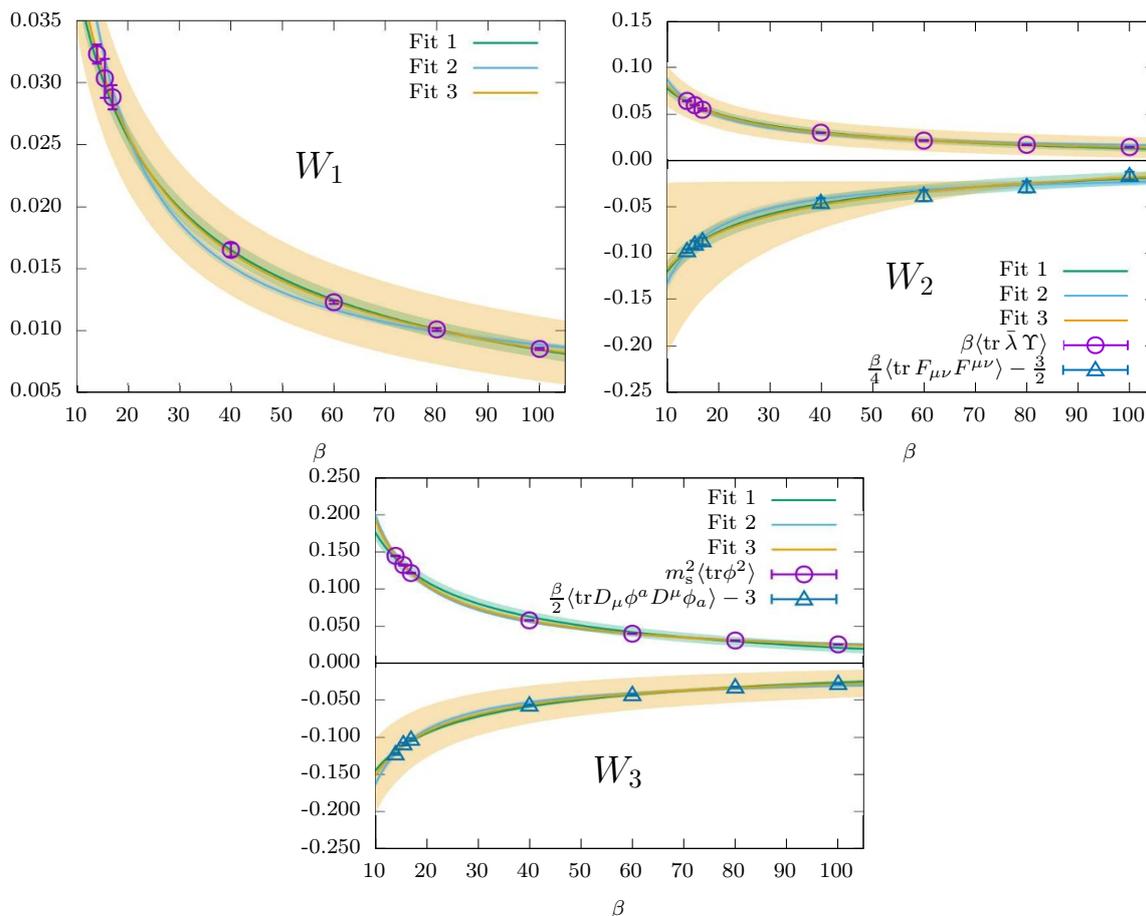
Figure 7. Ward identity W_1 and various terms contributing to the identities W_2 and W_3 in (4.4) for different values of β together with three different fits used for the continuum extrapolation. The theoretical value in the supersymmetric continuum limit for W_1 is zero.

we give W^∞ for W_1, the sum of the extrapolated components of W_2 and W_3 and the sum of these values for W_{B}. From the three fit functions we can estimate a systematic error coming from the choice of a particular fit function. This error alleviates our bias in choosing such a function. The *weighted average* takes into consideration the goodness of the fits. The Ward identities clearly point to the restoration of supersymmetry in the continuum limit, indicating also no sign of spontaneous susy breaking.

5 Mass spectrum

In order to determine the mass spectrum of the theory, we first perform the infinite volume limit, then the chiral limit and finally the continuum limit. For the infinite volume limit we study the dependence of the mass of the lightest state on the size of the system in order to locate a κ- and β-range where the results are (almost) insensitive to the volume. Then we simulate the theory at a fixed lattice volume for different values of the hopping parameter κ and extrapolate the results to the critical value $\kappa_{\mathrm{c}}(\beta)$, where the gluino becomes massless.
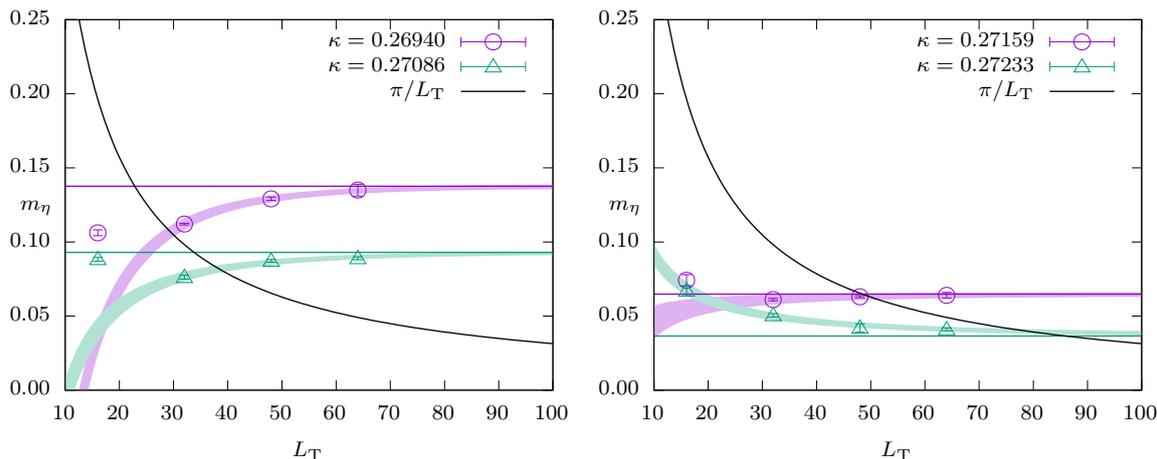
Figure 8. Infinite volume extrapolation for the mass of the η-meson at $\beta = 14$ and different values of the hopping parameter κ compared to the smallest lattice momentum π/L_{T}. The horizontal lines indicate the infinite volume mass m.

Finally we repeat the simulations for three different values of the gauge coupling β and try to extrapolate the results to $\beta \to \infty$.

5.1 Volume dependence

The finite volume dependency of bound states is given by [77, 78]

$$m_L = m - \frac{c}{L}\exp\left(-\frac{L}{L_0}\right), \tag{5.1}$$

where m_L is the mass at a finite lattice with spatial length L and m the mass in the infinite volume limit. The parameter L_0 represents the scale at which finite volume effects set in. In order to eliminate this fit parameter, we relate it to the infinite volume mass of the lightest particle, i.e. $L_0 = \pi/m_\eta$. The η-meson ground state mass m_L is shown for $\beta = 14$ and four different values of κ in figure 8. We observe two different kinds of behaviour. For $\kappa = 0.26940, 0.27086$ and 0.27159 the mass is monotonously increasing for $L_{\mathrm{T}} \geq 32$. For $\kappa = 0.27233$ it is monotonous decreasing. The explanation is that in the last case the infinite volume mass of $0.0365(14)$ is much smaller than the lattice cutoff π/L_{T} for all lattices. If the mass gets close to the lattice cutoff, we get back the monotonously increasing function. Nevertheless, we observe that the fit function works well for all cases and yields reliable results for the infinite volume mass. For the largest L_{T} value the mass m_L is within statistical errors the same as the infinite volume mass m. Thus we will restrict ourselves to this lattice size for the spectroscopy.

5.2 Mesons

We have calculated the π-, η- and f-meson correlation function (see appendix B) for different values of the hopping parameter κ. In figure 9 we show our results for two values of $\kappa \leq \kappa_{\mathrm{c}}$. For the larger value $\kappa = 0.26903$ the masses are slightly above the lattice momentum cutoff. First of all we observe that the π- and the η-meson correlation functions are
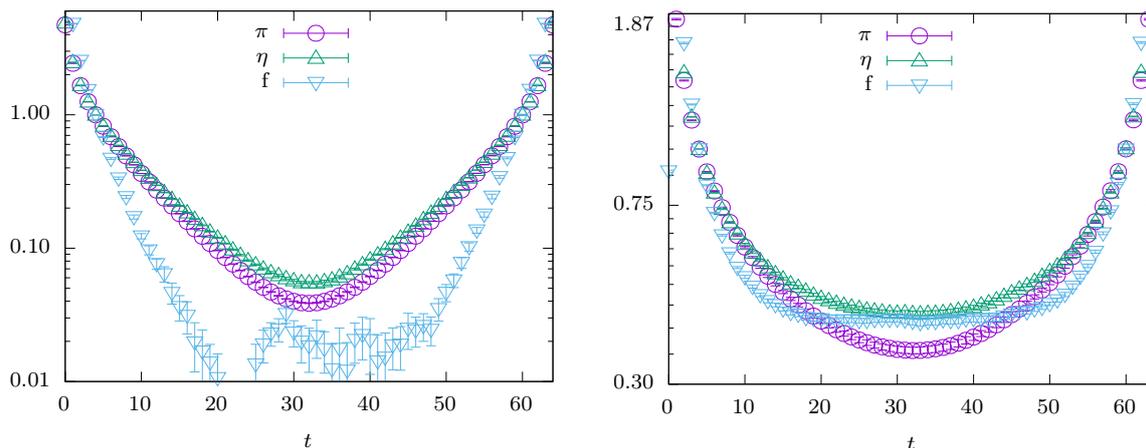
Figure 9. The η-,π- and f-meson correlation functions $C(t)$ as function of the temporal extend t are shown for $\beta = 17$ and $\kappa = 0.26655$ (left) and $\kappa = 0.26903$ (right).
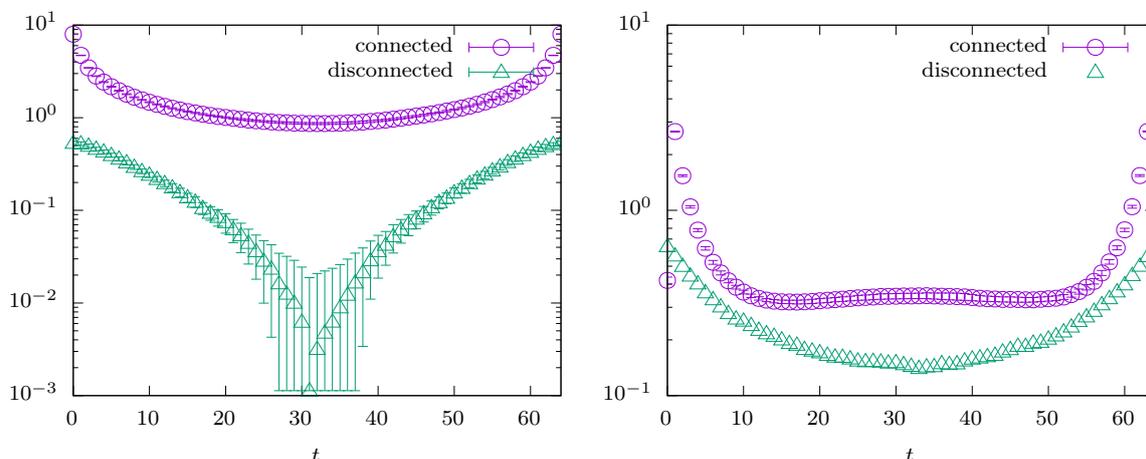

Figure 10. Connected and disconnected part of the η-meson (left) and f-meson (right) correlation function $C(t)$ as function of the temporal extend t for $\beta = 17$ and $\kappa = 0.26903$.

very similar for all values of κ considered and for intermediate values of t. For even larger t, the π meson correlation function decreases faster than the one for the η meson. Thus the ground state of the latter must be lighter. As the π ground state mass becomes zero in the chiral limit, the same will be true for the η-meson.

Next we observe that the correlation functions for the f- and the η-meson become degenerate in the chiral limit. This suggests, that indeed both mesons form a multiplet in the chiral limit, independent of the restoration of susy in the continuum limit. To further investigate this behaviour we study the connected and the disconnected contributions to the correlation functions. Recall, that the pion correlation function is defined as the connected part of the η-meson correlation function. In figure 10 we depicted the two contributions to the correlation functions for the η-meson (left) and the f-meson (right). For the η-meson we find that the connected part is at least one order of magnitude larger than the disconnected part and thus the η- and the π-meson correlation function are hard to distinguish. With

$\beta = 14.0$						
κ	0.26940	0.27086	0.27122	0.27159	0.27196	0.27233
m_η	0.135(4)	0.089(1)	0.076(1)	0.064(2)	0.053(1)	0.041(1)
$m_{\rm f}$	0.359(7)	0.247(4)	0.254(3)	0.074(2)	0.053(1)	0.046(2)
m_{η^*}	0.382(113)	0.347(30)	0.313(39)	0.287(31)	0.319(24)	0.318(29)
$m_{{\rm f}^*}$	-	-	-	0.509(7)	0.475(10)	0.471(9)
$\beta = 15.5$						
κ	0.26767	0.26911	0.26947	0.26983	0.27020	0.27056
m_η	0.130(2)	0.081(2)	0.074(1)	0.060(1)	0.047(1)	0.036(1)
$m_{\rm f}$	0.362(5)	0.275(4)	0.140(5)	0.059(1)	0.052(1)	0.037(1)
m_{η^*}	0.412(72)	0.281(33)	0.357(27)	0.318(22)	0.301(19)	0.302(26)
$m_{{\rm f}^*}$	-	-	0.656(23)	0.442(3)	0.504(8)	0.459(4)
$\beta = 17.0$						
κ	0.26655	0.26779	0.26810	0.26841	0.26872	0.26903
m_η	0.116(1)	0.076(1)	0.062(2)	0.054(1)	0.043(1)	0.034(2)
$m_{\rm f}$	0.335(2)	0.094(2)	0.064(3)	0.052(4)	0.030(1)	0.034(1)
m_{η^*}	0.407(42)	0.353(24)	0.285(32)	0.305(24)	0.295(23)	0.278(25)
$m_{{\rm f}^*}$	-	0.473(4)	0.434(5)	0.437(4)	0.402(4)	0.433(4)

Table 8. Masses of the η- and f-meson ground and excited states.

increasing t (but $2t \leq N_T$) the disconnected part gets even smaller. But despite of this we can still disentangle two slightly different masses in our simulations. Only in the chiral limit will η and π both become massless. For the f-meson the situation is different: the connected and disconnected contributions are roughly of equal size over the whole t range. Hence a observed degeneracy between η-meson and f-meson correlation functions is nontrivial. We determined the ground state and excited state masses of both mesons. The results are depicted in table 8 as well as in figure 11.

We see that the mass of the η-meson ground state depends linearly on the fermion mass $m_{\rm f}$. In fact, the zero crossing almost exactly hits the critical $m_{\rm f}^{\rm c}$. Thus m_η is proportional to $m_{\rm f} - m_{\rm f}^{\rm c}$ and will vanish in the chiral limit. For the f meson, a linear dependence is seen only for a fermion mass close to the critical fermion mass, where the latter is the same as for the pion. This behaviour is more pronounced for the larger values of β. Thus in the chiral limit we find the same ground state masses for the f-meson and the η-meson.

For the excited states we can not make a comparably strong statement, since it is more difficult to extract their masses. For the η-meson we used a fit with three masses, which agrees rather well over the whole t-range with the correlator. As the largest mass was above 1, it is heavily afflicted with discretization artifacts and thus discarded. Hence only the masses of the ground states and first excited states are given in table 8. We compared
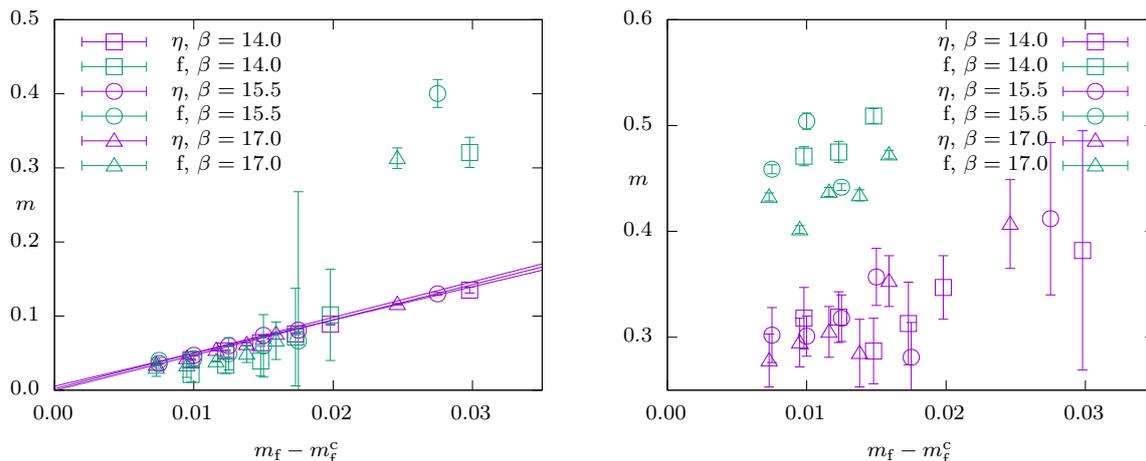
Figure 11. Ground (left) and excited (right) state masses of the η- and f-meson as function of the pion mass squared for $\beta = 14$, 15.5 and 17. For the η ground states we show linear fits.

these results with the effective mass extracted from the corresponding correlation function. For both η and f we find one plateau corresponding to their ground state mass. Using the so obtained values to fit the correlation functions for small t leads to the values of the first excited state of the f meson, given in table 8. Unfortunately this method of determination leads to a large unknown systematic error. Comparing the results for different values of β, we observe that the mass of the excited f-meson decreases slowly with increasing β. Thus it could approach the mass of the excited η meson in the continuum limit. Unfortunately our results do not allow for an unambiguous extrapolation to the chiral limit, preventing also the continuum extrapolation.

5.3 Gluino-glueball

In the four-dimensional multiplet we have two gluino-glueball particles, which differ by their transformation under parity. As interpolating fermionic operator we use

$$O_{GG} = \Sigma_{\mu\nu} F^{\mu\nu} \lambda \tag{5.2}$$

where the $F^{\mu\nu}$ is approximated on the lattice by the clover plaquette. Although the projectors on a definite parity quantum number are $P_\pm = (1 \pm \Gamma_0)/2$ it is more convenient to project on periodic (S) and antiperiodic (A) correlation functions

$$C_A(t) = \left\langle O_{GG}(t) O_{GG}^\dagger(0) \right\rangle, \qquad C_S(t) = \left\langle O_{GG}(t) \Gamma_0 O_{GG}^\dagger(0) \right\rangle. \tag{5.3}$$

All other contractions over Γ-matrices can be written as a linear combination of these two correlation functions, as expected for two independent physical states.

The determination of masses on larger lattices is only possible with the help of gauge field smearing. We introduce the smearing level $S = \text{steps} \times \text{parameter}$, where 'steps' are the amount of smearing steps and 'parameter' is the smearing parameter for these steps. The correlation functions $C_S(t)$ for different smearing levels are shown in figure 12 (left panel). Even for a large number of smearing steps the signal still improves. Table 9 shows

S	12	40	120	200	300	400
m_A	0.486(11)	0.360(7)	0.320(5)	0.310(5)	0.289(12)	0.287(10)
m_S	0.410(10)	0.313(5)	0.265(2)	0.252(3)	0.246(3)	0.243(3)

Table 9. Extracted masses for different smearing levels S for the symmetric and antisymmetric gluino-glueball states for $\beta = 17$ and $m_f = -0.1415$.
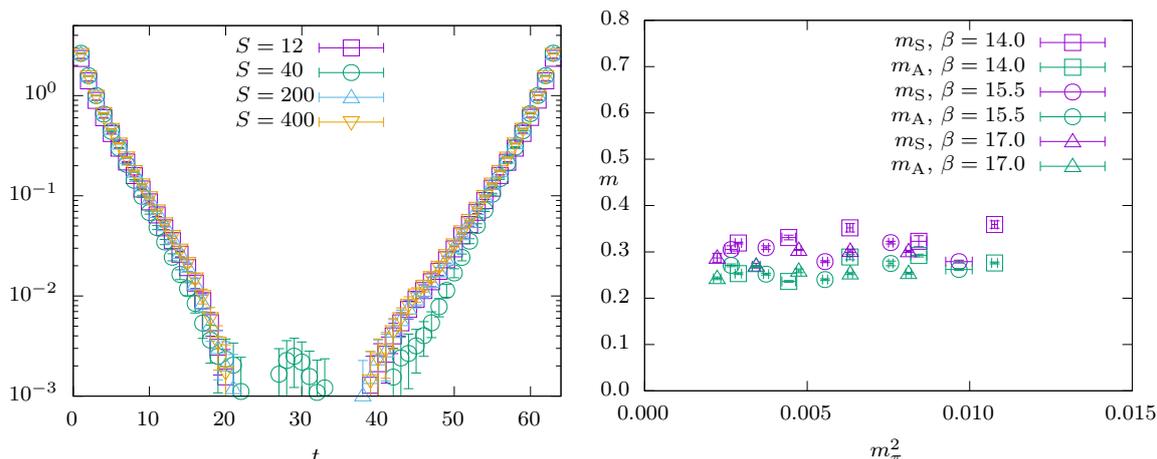

Figure 12. Left: gluino-glue correlation function $C(t)$ as function of the temporal extend t at $\beta = 17$ and $m_f = -0.1350$ for different smearing levels S. Right: gluino-glue mass as a function of the squared pion mass.

our results for $\beta = 17$ and $m_f = -0.1415$. For both masses, we see a nice convergence with increasing smearing. This behaviour is even seen for large smearing levels ($S = 400$). Both masses m_A and m_S converge to the same value as expected in a parity symmetric theory. Furthermore the mass depends only very weakly on the gauge coupling β and the bare fermion mass m_f (see figure 12, right panel).

Comparing with the masses of the mesons, we find that the gluino-glueballs have comparable masses as the excited state of the η-meson. An explanation for this unexpected behavior could be, that the first excited state of the gluino-glueball dominates the correlation function over a long t-range, such that the ground state contribution is not visible on our lattice sizes. To see whether this is the case, we applied this large amount of smearing ($S = 400$), but we did not observe any sign of a lighter particle in this channel. Thus an alternative explanation could be, that we indeed detected the ground state of the gluino-glueball. But then one must explain why the gluino-glueball forms a multiplet with the excited mesons and not the mesons in their ground states. The fermionic state in the VY-multiplet is a mixture of the gluino-glue and a gluino-scalarball. Possibly the gluino-scalarball has a lighter mass. Unfortunately, also with a large amount of smearing for the scalar field, we are not able to obtain an estimate for its mass.
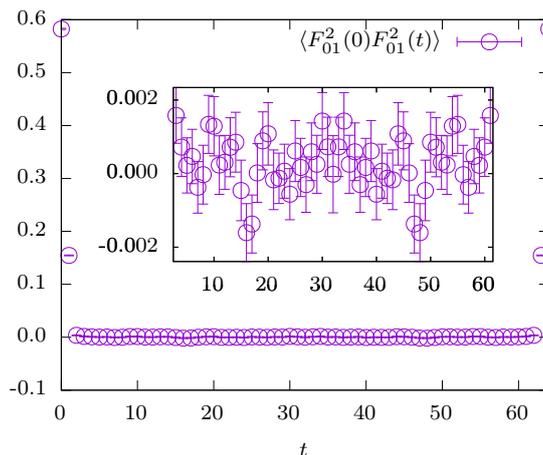
Figure 13. Glueball correlation function $C(t)$ as function of the temporal extend t for $\beta = 17$ and $m_{\mathrm{f}} = -0.074$.

5.4 Glue- and scalarballs

The second multiplet of bound states consists of glue-, scalar- and glue-scalarballs. The correlation functions of the corresponding interpolating operators show no correlation at all for large distances. For the glueball, this is shown in figure 13. The only nonzero values of the correlation function are at distances $t = 0, 1, 63$ and 64. A similar behavior is seen in pure Yang-Mills theory on a two-dimensional lattice. Indeed, with Migdals prescription [79] one obtains for the correlation function of the glueball operator $G(x)$ in this theory

$$\langle G(x)G^{\dagger}(y)\rangle = C_{\mathrm{G}} = \mathrm{const.} \tag{5.4}$$

This holds true in case the supports of the interpolating operators are disjunct. Hence the correlation function of glueballs will show only a correlation between time slices with distance less than the diameter A_G of the support of $G(x)$. We observe the very same behaviour in the supersymmetric theory in figure 13, where the diameter is two. In the continuum limit, the physical diameter shrinks to zero and the expectation value is constant in the whole spacetime volume. Furthermore one can show, that this value goes to zero and the glueball decouples completely from the theory. This lattice result is in agreement with the analytical result presented in [80].

Since we use smearing of sources and sinks in our analysis, it maybe instructive to study the effect of smearing on the correlation function of glueballs. Every smearing step increases the diameter A_{G}, and thus induces more artificial correlations between the lattice points, which are uncorrelated without smearing. The results can be seen in figure 14, where we compare pure Yang-Mills theory (left) to susy Yang-Mills theory (right). In both cases we observe more nonzero values in the correlation functions for higher smearing levels, as expected. Smearing effects can also be seen in the effective mass: in both theories it is an ever increasing function of the distance for all values of the smearing level. We conclude that, similarly as in pure YM-theory in two dimensions, there is no correlation for glueballs. In other words, the glueball completely decouples from the $\mathcal{N} = (2, 2)$ SYM
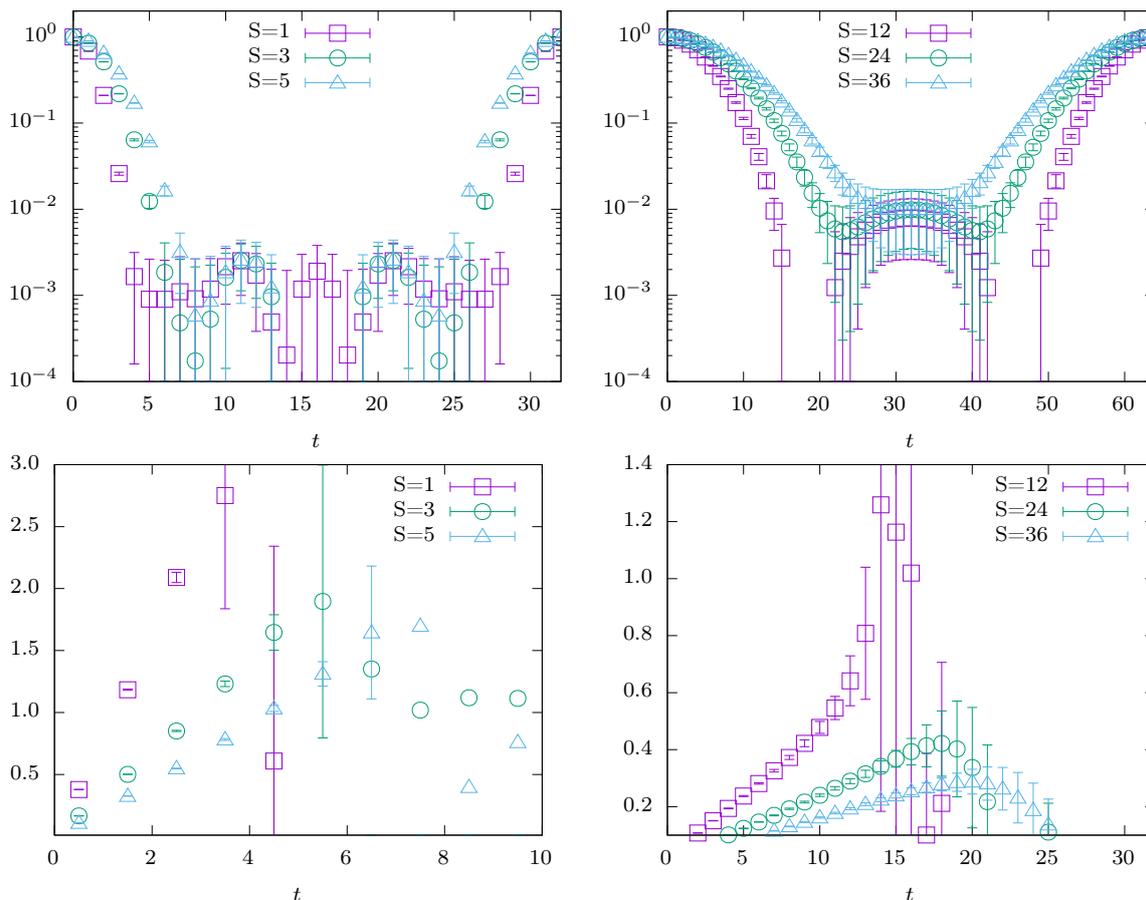
Figure 14. Comparison between the glueball correlation function $C(t)$ as function of the temporal extend t for the two-dimensional Yang-Mills theory (left) and the two-dimensional Super Yang-Mills theory (right) for different smearing levels S. In the bottom row we plot the effective mass.

theory in two dimensions. Similarly we could not detect any correlations in the scalarball and glue-scalarball correlator functions. Since they should form a super-multiplet with the glueball, they will decouple from the theory as well. The additional gluino-glueball state in the super-multiplet will also show no correlations, and thus is not seen in our simulations.

6 Conclusions

In our work, we simulated the two-dimensional $\mathcal{N} = (2,2)$ SYM lattice-theory in a conventional approach without twisting. The simulation could be afflicted with two potentially serious problems common in gauge theories with extended supersymmetry: flat directions and a sign problem. In the present work we demonstrate that these problems do not arise for all parameters which are relevant to approach the supersymmetric continuum limit. As concerning the sign problem, this is related to the absence of the sign problem in the $\mathcal{Q}$-exact formulation of the continuum theory [81].

When studying various Ward identities, we did observe that they are rather insensitive to the bare mass of the scalars $m_{\rm s}$, as long as the latter is in the vicinity of the

particle	m	m^*
a-η	$0.034(2) \to 0$	$0.278(25)$
a-f	$0.034(1) \to 0$	$0.433(4)$
gluino-glueball	—	$0.243(3)/0.287(10)$

Table 10. We observe the formation of a massive VY-multiplet while the ground states are massless. The FGS-multiplet decouples from the theory.

(all-loop) perturbative value in the supersymmetric continuum model, which is given by $m_{\mathrm{s}}^2 = 0.659\,482\,55(8)$. Away from the continuum limit this may not be the optimal choice. Spotting an observable, which allows for further fine-tuning of the scalar mass on the lattice could perhaps improve the results and would allow for more accurate predictions. But such an improvement is probably not easy to achieve since our results are stable and reliable. They do not depend on the scalar mass in the vicinity of the above value and thus a further fine-tuning of m_{s} does not help much.

The restoration of supersymmetry is observed in the chiral limit. Since the fermion mass is not a relevant coupling (contrary to the situation in four dimensions) this may come as a surprise. But generally speaking fine-tuning of an irrelevant coupling may be helpful away from criticality. In any case, the result confirms the assumption, that supersymmetry is recovered in the chiral limit, similarly as in the four-dimensional mother-theory. But the spectrum of bound states looks different than in the four-dimensional $\mathcal{N} = 1$ theory. We found a massless multiplet — the dimensionally reduced Veneziano-Yankielowicz multiplet — which contains the mesons, while the Farrar-Gabadadze-Schwetz multiplet decouples from the theory (see table 10). The mass of the lightest gluino-glueball seen in the simulations is still a bit ambiguous. Within errors its mass is equal to that of the excited mesons. We believe we could not follow the corresponding correlation function for large enough t-values, in order to disentangle the signals from the ground state and excited state. Probably we did only see the excited gluino-glueball which forms a multiplet with the excited meson states. If this is true, then finding the missing ground state of the gluino-glueball may be as difficult as finding a needle in a haystack.

In this work we could not see any screening of static charges in the fundamental representation, although the dynamical fermions are in the adjoint. Instead our accurate simulations indicate that $\mathcal{N} = (2, 2)$ and $\mathcal{N} = (1, 1)$ SYM theory in two dimensions both confine static charges in the fundamental representation. At least the result for the $\mathcal{N} = (1, 1)$ theory with Majorana fermions seems to be in conflict with analytic results in [66]. Clearly, this clash of numerical simulations with analytical results should be resolved in future works.

In future studies we intend to study the phase structure of the $\mathcal{N} = (2, 2)$ SYM theory as well as related systems with more supersymmetries. It would be interesting to measure the two independent holonomies (Wilson loops with windings) on the two-torus and their dependence on the geometry of the torus. This way one could first compare with results obtained with $\mathcal{Q}$-exact formulations for $\mathcal{N} = (8, 8)$ SYM theory [82] and furthermore extend to systems with less supersymmetry where no $\mathcal{Q}$-exact formulation exists. Since we did

not encounter any sign problems for $\kappa < \kappa_c$ and since the flat directions are stabilized, we should be able to accurately localize the expected phases and phase-transition lines in two-dimensional SYM with extended supersymmetry.

Acknowledgments

A   Exact lattice Ward identities

In the main body of the text we studied the violation of several Ward identities due to lattice artifacts. Thereby we neglected contributions stemming from m_f and m_s deviating from their critical values. Here we derive lattice Ward identities without any approximation. The application of the lattice supersymmetry transformations (4.1) to the lattice Lagrangian results in

$$
\begin{aligned}
\bar{Q}^\alpha \mathcal{L}_\mathrm{lat} &= \frac{\beta}{2} \left\{ \partial_\mu s_\mu{}^\alpha - 2m_\mathrm{f} \left(\Gamma_{MN} \right)^{\alpha\beta} F^{MN} \lambda_\beta \right\} + 2m_\mathrm{s}^2 \left(\Gamma_{m+1} \right)^\alpha{}_\beta \lambda^\beta \phi^m + X_\mathrm{S} \\
&= \frac{\beta}{2} \left\{ \partial_\mu s_\mu^\alpha - m_\mathrm{f} \chi_\mathrm{f}^\alpha \right\} + m_\mathrm{s}^2 \chi_\mathrm{s}^\alpha + X_\mathrm{S},
\end{aligned}
\tag{A.1}
$$

with

$$
\chi_\mathrm{f}^\alpha = 2 \operatorname{tr} \left(\Gamma_{MN}^{\alpha\beta} F^{MN} \lambda_\beta \right) \quad \text{and} \quad \chi_\mathrm{s}^\alpha = 2 \operatorname{tr} \left(\Gamma_{m+1}^{\alpha\beta} \lambda_\beta \phi^m \right).
\tag{A.2}
$$

The contributions χ^α originate from the fermion and scalar mass terms introduced in the lattice Lagrangian. As pointed out previously the supercurrent s_μ^α vanishes after summation over the lattice sites. The term X_S originates from the lattice regularisation and is of order $\mathcal{O}(a)$. Clearly, at tree-level supersymmetry is restored in the continuum limit for the critical values $m_\mathrm{f}^\mathrm{c} = m_\mathrm{s}^\mathrm{c} = 0$. At one-loop a finite scalar mass is generated due to different lattice momenta of bosons and fermions. Furthermore, the Wilson term in the fermion operator gives rise to a nonzero critical fermion mass. In the continuum limit, no further corrections are generated at higher loop order such that $m_\mathrm{f}^\mathrm{c} \to 0$. In order to compensate for the shifts at finite lattice spacing one adds counter-terms to the tree-level lattice action and ends up with the full quantum lattice Ward identity (4.3). The scalar mass counter-term must also be included in the Ward identity W_3 and the bosonic Ward identity because they contain the kinetic term for the scalar fields. Thus, the set of lattice Ward identities read

$$
\begin{aligned}
W_\mathrm{B} &= \beta V^{-1} \langle S_\mathrm{B} \rangle + m_\mathrm{s}^2 \langle \operatorname{tr} \phi^2 \rangle + \beta \langle \operatorname{tr} \bar{\lambda} \, \Gamma^{MN} F_{MN} \, \Theta \rangle \to \frac{9}{2}, \\
W_3 &= \frac{\beta}{2} \langle \operatorname{tr} D_\mu \phi^a D^\mu \phi_a \rangle + m_\mathrm{s}^2 \langle \operatorname{tr} \phi^2 \rangle + 2\beta \left\langle \operatorname{tr} \bar{\lambda} \, \Gamma^{\mu m} D_\mu \phi_m \, \Theta \right\rangle \to 3, \\
W_2 &= \frac{\beta}{4} \langle \operatorname{tr} F_{\mu\nu} F^{\mu\nu} \rangle + \beta \langle \operatorname{tr} \bar{\lambda} \Upsilon \rangle + \beta \langle \operatorname{tr} \bar{\lambda} \, \Gamma^{\mu\nu} F_{\mu\nu} \Theta \rangle \to \frac{3}{2}, \\
W_1 &= \frac{\beta}{2} \langle \operatorname{tr} [\phi_1, \phi_2]^2 \rangle - \beta \langle \operatorname{tr} \bar{\lambda} \, \Upsilon \rangle + \beta \langle \operatorname{tr} \bar{\lambda} \, \Gamma^{mn} [\phi_m, \phi_n] \, \Theta \rangle \to 0,
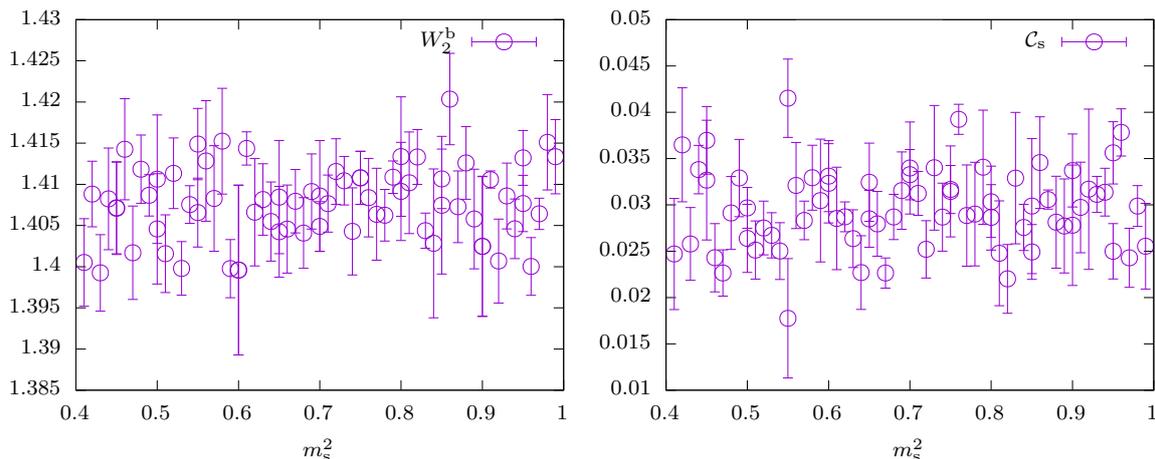\end{aligned}
\tag{A.3}
$$

Figure 15. On the left we see the term W_2^{b} and on the right the term $\mathcal{C}_{\mathrm{s}}$.

where we used the abbreviations

$$\Theta = \left(m_{\mathrm{s}}^2 - (m_{\mathrm{s}}^{\mathrm{c}})^2\right)\chi_{\mathrm{s}} - (m_{\mathrm{f}} - m_{\mathrm{f}}^{\mathrm{c}})\chi_{\mathrm{f}}, \quad \Upsilon = \frac{\mathrm{i}}{8}\big(\Gamma_2\left[\phi_1, \lambda\right] + \Gamma_3\left[\phi_2, \lambda\right]\big). \tag{A.4}$$

Near the supersymmetric continuum limit, lattice artifacts should be sufficiently suppressed such that the breaking of Ward identities originate from the missing fine-tuning of $m_{\mathrm{f}}^{\mathrm{c}}$ and $m_{\mathrm{s}}^{\mathrm{c}}$. Since we anyway use the π-mass to fine-tune $m_{\mathrm{f}}^{\mathrm{c}}$ we will focus on the fine-tuning of $m_{\mathrm{s}}^{\mathrm{c}}$ in what follows. We will show this fine-tuning approach for the Ward-identity W_2. The results for the other identities are very similar.

First we introduce W_2^{b} and the correction terms $\mathcal{C}_{\mathrm{s}}$ and $\mathcal{C}_{\mathrm{f}}$

$$W_2^{\mathrm{b}} = \beta\langle\frac{1}{4}\operatorname{tr}F_{\mu\nu}F^{\mu\nu} + \operatorname{tr}\bar{\lambda}\Upsilon\rangle, \quad \mathcal{C}_{\mathrm{s}} = \langle\operatorname{tr}\bar{\lambda}\,\Gamma^{\mu\nu}F_{\mu\nu}\chi_{\mathrm{s}}\rangle, \quad \mathcal{C}_{\mathrm{f}} = \beta\langle\operatorname{tr}\bar{\lambda}\,\Gamma^{\mu\nu}F_{\mu\nu}\chi_{\mathrm{f}}\rangle, \tag{A.5}$$

which enter the Ward identity W_2 of interest,

$$W_2 = W_2^{\mathrm{b}} + \left(m_{\mathrm{s}}^2 - (m_{\mathrm{s}}^{\mathrm{c}})^2\right)\mathcal{C}_{\mathrm{s}} + (m_{\mathrm{f}} - m_{\mathrm{f}}^{\mathrm{c}})\mathcal{C}_{\mathrm{f}}. \tag{A.6}$$

Now we simulate the gauge theory for a set of values m_{s}^2 near the one-loop value 0.6594826 and measure the expectation values W_2^{b}, $\mathcal{C}_{\mathrm{s}}$ and $\mathcal{C}_{\mathrm{f}}$. Note that m_{s} and m_{f} are the masses used to generate the ensemble, whereas the trial mass $m_{\mathrm{s}}^{\mathrm{c}}$ only enters via the operators defining the Ward identities. Next we should extract a trial mass for which $W_2 \approx \frac{3}{2}$ for all m_{s} near the critical value. Note that the extracted $m_{\mathrm{s}}^{\mathrm{c}}$ could deviate from the one-loop results due to lattice artifacts.

Figure 15 clearly shows that W_2^{b} and $\mathcal{C}_{\mathrm{s}}$ do not depend sensitively on m_{s} near the critical one-loop value. The same holds true for $\mathcal{C}_{\mathrm{f}}$, which is not shown in the figure. This means that it is difficult to find any deviations of $m_{\mathrm{s}}^{\mathrm{c}}$ from its known continuum one-loop value. But since the correction terms $\mathcal{C}_{\mathrm{s}}$ and $\mathcal{C}_{\mathrm{f}}$ in (A.6) are two orders of magnitude smaller than W_2^{b} we may safely neglect the lattice correction Θ if we are close to the critical masses, which we ensure by extrapolating to the chiral limit and using 0.6594826. This leads to the final set of approximate Ward identities (4.4) which are measured in our simulations.

B   Meson correlation functions

In order to extract meson masses, we measure the connected two-point functions of the operators $\bar{\lambda}_m \Gamma \lambda_n$,

$$C_{\Gamma,m,n}(x,y) = \left\langle \left(\bar{\lambda}_m \Gamma \lambda_n\right)_x \left(\bar{\lambda}_n \Gamma \lambda_m\right)_y \right\rangle - \left\langle \left(\bar{\lambda}_m \Gamma \lambda_n\right)_x \right\rangle \left\langle \left(\bar{\lambda}_n \Gamma \lambda_m\right)_y \right\rangle \qquad \text{(B.1)}$$

with $\Gamma = \mathbb{1}$ for the scalar mesons and $\Gamma = \Gamma_5$ for the axial mesons. The indices m, n are flavour indices. In a two-flavour setup, the f-meson mass is extracted from the decay of $C_{\mathrm{f}} = C_{\mathbb{1},1,1}$, the η-meson mass from $C_\eta = C_{\Gamma_5,1,1}$ and the pion mass from $C_\pi = C_{\Gamma_5,1,2}$. After integration over the fermions, we obtain

$$\begin{aligned} C_{\Gamma,m,n}(x,y) = &\left\langle \mathrm{tr}\left(\Delta_{x,x}^{mn}\Gamma\right)\mathrm{tr}\left(\Delta_{y,y}^{nm}\Gamma\right) - \mathrm{tr}\left(\Delta_{x,y}^{mm}\Gamma\Delta_{y,x}^{nn}\Gamma\right)\right\rangle \\ &- \left\langle \mathrm{tr}\left(\Delta_{x,x}^{mn}\Gamma\right)\right\rangle \left\langle \mathrm{tr}\left(\Delta_{y,y}^{nm}\Gamma\right)\right\rangle \end{aligned} \qquad \text{(B.2)}$$

with the fermion propagator Δ. In our simulations, only one fermion flavour is dynamic. The pion correlation function is therefore defined in a *partially quenched* setup which implies $\Delta^{11} = \Delta^{22} = \Delta$ and $\Delta^{1,2} = \Delta^{2,1} = 0$. We get for the different correlation functions

$$\begin{aligned} C_{\mathrm{f}}(x,y) &= \left\langle \mathrm{tr}\left(\Delta_{x,x}\right)\mathrm{tr}\left(\Delta_{y,y}\right) - \mathrm{tr}\left(\Delta_{x,y}\Delta_{y,x}\right)\right\rangle - \left\langle \mathrm{tr}\left(\Delta_{x,x}\right)\right\rangle\left\langle \mathrm{tr}\left(\Delta_{y,y}\right)\right\rangle , \\ C_\eta(x,y) &= \left\langle \mathrm{tr}\left(\Delta_{x,x}\Gamma_5\right)\mathrm{tr}\left(\Delta_{y,y}\Gamma_5\right) - \mathrm{tr}\left(\Delta_{x,y}\Gamma_5\Delta_{y,x}\Gamma_5\right)\right\rangle - \left\langle \mathrm{tr}\left(\Delta_{x,x}\Gamma_5\right)\right\rangle\left\langle \mathrm{tr}\left(\Delta_{y,y}\Gamma_5\right)\right\rangle , \\ C_\pi(x,y) &= \left\langle -\,\mathrm{tr}\left(\Delta_{x,y}\Gamma_5\Delta_{y,x}\Gamma_5\right)\right\rangle . \end{aligned} \qquad \text{(B.3)}$$

For a single flavour, the pion correlation function is therefore defined as the *connected* part of the η-meson correlation function, where connected refers to a diagramatical interpretation of traces over the fermion propagator.

Open Access. This article is distributed under the terms of the Creative Commons Attribution License ([CC-BY 4.0](#)), which permits any use, distribution and reproduction in any medium, provided the original author(s) and source are credited.

References

[1] A. Salam and J.A. Strathdee, *Supersymmetry and non-Abelian gauges*, *Phys. Lett.* **B 51** (1974) 353 [INSPIRE].

[2] S. Ferrara and B. Zumino, *Supergauge invariant Yang-Mills theories*, *Nucl. Phys.* **B 79** (1974) 413 [INSPIRE].

[3] D. Amati, K. Konishi, Y. Meurice, G.C. Rossi and G. Veneziano, *Nonperturbative aspects in supersymmetric gauge theories*, *Phys. Rept.* **162** (1988) 169 [INSPIRE].

[4] G. Veneziano and S. Yankielowicz, *An effective Lagrangian for the pure N = 1 supersymmetric Yang-Mills theory*, *Phys. Lett.* **B 113** (1982) 231 [INSPIRE].

[5] G.R. Farrar, G. Gabadadze and M. Schwetz, *The spectrum of softly broken N = 1 supersymmetric Yang-Mills theory*, *Phys. Rev.* **D 60** (1999) 035002 [`hep-th/9806204`] [INSPIRE].

[6] G.R. Farrar, G. Gabadadze and M. Schwetz, *On the effective action of N = 1 supersymmetric Yang-Mills theory*, *Phys. Rev.* **D 58** (1998) 015009 [hep-th/9711166] [INSPIRE].

[7] A. Feo, P. Merlatti and F. Sannino, *Information on the super Yang-Mills spectrum*, *Phys. Rev.* **D 70** (2004) 096004 [hep-th/0408214] [INSPIRE].

[8] G. Curci and G. Veneziano, *Supersymmetry and the lattice: a reconciliation?*, *Nucl. Phys.* **B 292** (1987) 555 [INSPIRE].

[9] J. Giedt, R. Brower, S. Catterall, G.T. Fleming and P. Vranas, *Lattice super-Yang-Mills using domain wall fermions in the chiral limit*, *Phys. Rev.* **D 79** (2009) 025015 [arXiv:0810.5746] [INSPIRE].

[10] M.G. Endres, *Dynamical simulation of N = 1 supersymmetric Yang-Mills theory with domain wall fermions*, *Phys. Rev.* **D 79** (2009) 094503 [arXiv:0902.4267] [INSPIRE].

[11] JLQCD collaboration, *Lattice study of 4d N = 1 super Yang-Mills theory with dynamical overlap gluino*, PoS(LATTICE2011)069 (2011) [arXiv:1111.2180] [INSPIRE].

[12] I. Montvay, *SUSY on the lattice*, *Nucl. Phys. Proc. Suppl.* **63** (1998) 108 [hep-lat/9709080] [INSPIRE].

[13] DESY-MUNSTER collaboration, *Monte Carlo simulation of SU(2) Yang-Mills theory with light gluinos*, *Eur. Phys. J.* **C 11** (1999) 507 [hep-lat/9903014] [INSPIRE].

[14] DESY-MUNSTER-ROMA collaboration, *The supersymmetric Ward identities on the lattice*, *Eur. Phys. J.* **C 23** (2002) 719 [hep-lat/0111008] [INSPIRE].

[15] I. Montvay, *Supersymmetric Yang-Mills theory on the lattice*, *Int. J. Mod. Phys.* **A 17** (2002) 2377 [hep-lat/0112007] [INSPIRE].

[16] G. Münster and H. Stüwe, *The mass of the adjoint pion in N = 1 supersymmetric Yang-Mills theory*, *JHEP* **05** (2014) 034 [arXiv:1402.6616] [INSPIRE].

[17] G. Bergner, P. Giudice, G. Münster, S. Piemonte and D. Sandbrink, *Phase structure of the N = 1 supersymmetric Yang-Mills theory at finite temperature*, *JHEP* **11** (2014) 049 [arXiv:1405.3180] [INSPIRE].

[18] G. Bergner and S. Piemonte, *Compactified N = 1 supersymmetric Yang-Mills theory on the lattice: continuity and the disappearance of the deconfinement transition*, *JHEP* **12** (2014) 133 [arXiv:1410.3668] [INSPIRE].

[19] G. Bergner, P. Giudice, G. Münster, I. Montvay and S. Piemonte, *The light bound states of supersymmetric SU(2) Yang-Mills theory*, *JHEP* **03** (2016) 080 [arXiv:1512.07014] [INSPIRE].

[20] S. Ali et al., *The light bound states of N = 1 supersymmetric SU(3) Yang-Mills theory on the lattice*, *JHEP* **03** (2018) 113 [arXiv:1801.08062] [INSPIRE].

[21] M. Steinhauser, A. Sternbeck, B. Wellegehausen and A. Wipf, *Spectroscopy of four-dimensional N = 1 supersymmetric SU(3) Yang-Mills theory*, *EPJ Web Conf.* **175** (2018) 08022 [arXiv:1711.05086] [INSPIRE].

[22] H. Suzuki and Y. Taniguchi, *Two-dimensional N = (2, 2) super Yang-Mills theory on the lattice via dimensional reduction*, *JHEP* **10** (2005) 082 [hep-lat/0507019] [INSPIRE].

[23] H. Fukaya, I. Kanamori, H. Suzuki and T. Takimi, *Numerical results of two-dimensional N = (2, 2) super Yang-Mills theory*, PoS(LATTICE2007)264 (2007) [arXiv:0709.4076] [INSPIRE].

[24] E. Witten, *Bound states of strings and p-branes*, *Nucl. Phys.* **B 460** (1996) 335 [hep-th/9510135] [ɪɴSPIRE].

[25] H. Fukaya, I. Kanamori, H. Suzuki, M. Hayakawa and T. Takimi, *Note on massless bosonic states in two-dimensional field theories*, *Prog. Theor. Phys.* **116** (2007) 1117 [hep-th/0609049] [ɪɴSPIRE].

[26] F. Antonuccio, H.C. Pauli, S. Pinsky and S. Tsujimaru, *DLCQ bound states of N = (2, 2) super Yang-Mills at finite and large N*, *Phys. Rev.* **D 58** (1998) 125006 [hep-th/9808120] [ɪɴSPIRE].

[27] M. Harada, J.R. Hiller, S. Pinsky and N. Salwen, *Improved results for N = (2, 2) super Yang-Mills theory using supersymmetric discrete light-cone quantization*, *Phys. Rev.* **D 70** (2004) 045015 [hep-th/0404123] [ɪɴSPIRE].

[28] K. Hori and D. Tong, *Aspects of non-Abelian gauge dynamics in two-dimensional N = (2, 2) theories*, *JHEP* **05** (2007) 079 [hep-th/0609032] [ɪɴSPIRE].

[29] S. Catterall, R.G. Jha and A. Joseph, *Nonperturbative study of dynamical SUSY breaking in N = (2, 2) Yang-Mills theory*, *Phys. Rev.* **D 97** (2018) 054504 [arXiv:1801.00012] [ɪɴSPIRE].

[30] T. Kastner, G. Bergner, S. Uhlmann, A. Wipf and C. Wozar, *Two-dimensional Wess-Zumino models at intermediate couplings*, *Phys. Rev.* **D 78** (2008) 095001 [arXiv:0807.1905] [ɪɴSPIRE].

[31] A.G. Cohen, D.B. Kaplan, E. Katz and M. Ünsal, *Supersymmetry on a Euclidean space-time lattice. 2. Target theories with eight supercharges*, *JHEP* **12** (2003) 031 [hep-lat/0307012] [ɪɴSPIRE].

[32] S. Catterall, *A geometrical approach to N = 2 super Yang-Mills theory on the two dimensional lattice*, *JHEP* **11** (2004) 006 [hep-lat/0410052] [ɪɴSPIRE].

[33] F. Sugino, *A lattice formulation of super Yang-Mills theories with exact supersymmetry*, *JHEP* **01** (2004) 015 [hep-lat/0311021] [ɪɴSPIRE].

[34] S. Matsuura and F. Sugino, *Lattice formulation for 2d N = (2, 2), (4, 4) super Yang-Mills theories without admissibility conditions*, *JHEP* **04** (2014) 088 [arXiv:1402.0952] [ɪɴSPIRE].

[35] S. Catterall, *Simulations of N = 2 super Yang-Mills theory in two dimensions*, *JHEP* **03** (2006) 032 [hep-lat/0602004] [ɪɴSPIRE].

[36] S. Catterall, *First results from simulations of supersymmetric lattices*, *JHEP* **01** (2009) 040 [arXiv:0811.1203] [ɪɴSPIRE].

[37] I. Kanamori and H. Suzuki, *Restoration of supersymmetry on the lattice: two-dimensional N = (2, 2) supersymmetric Yang-Mills theory*, *Nucl. Phys.* **B 811** (2009) 420 [arXiv:0809.2856] [ɪɴSPIRE].

[38] H. Suzuki, *Two-dimensional N = (2, 2) super Yang-Mills theory on computer*, *JHEP* **09** (2007) 052 [arXiv:0706.1392] [ɪɴSPIRE].

[39] I. Kanamori and H. Suzuki, *Some physics of the two-dimensional N = (2, 2) supersymmetric Yang-Mills theory: lattice Monte Carlo study*, *Phys. Lett.* **B 672** (2009) 307 [arXiv:0811.2851] [ɪɴSPIRE].

[40] I. Kanamori, F. Sugino and H. Suzuki, *Observing dynamical supersymmetry breaking with euclidean lattice simulations*, *Prog. Theor. Phys.* **119** (2008) 797 [arXiv:0711.2132] [ɪɴSPIRE].

[41] D. Kadoh and H. Suzuki, *SUSY WT identity in a lattice formulation of 2D N = (2, 2) SYM*, *Phys. Lett.* **B 682** (2010) 466 [arXiv:0908.2274] [InSPIRE].

[42] T. Takimi, *Relationship between various supersymmetric lattice models*, *JHEP* **07** (2007) 010 [arXiv:0705.3831] [InSPIRE].

[43] P.H. Damgaard and S. Matsuura, *Lattice supersymmetry: equivalence between the link approach and orbifolding*, *JHEP* **09** (2007) 097 [arXiv:0708.4129] [InSPIRE].

[44] P.H. Damgaard and S. Matsuura, *Relations among supersymmetric lattice gauge theories via orbifolding*, *JHEP* **08** (2007) 087 [arXiv:0706.3007] [InSPIRE].

[45] M. Ünsal, *Twisted supersymmetric gauge theories and orbifold lattices*, *JHEP* **10** (2006) 089 [hep-th/0603046] [InSPIRE].

[46] D.B. Kaplan, *Recent developments in lattice supersymmetry*, *Nucl. Phys. Proc. Suppl.* **129** (2004) 109 [hep-lat/0309099] [InSPIRE].

[47] J. Giedt, *Deconstruction and other approaches to supersymmetric lattice field theories*, *Int. J. Mod. Phys.* **A 21** (2006) 3039 [hep-lat/0602007] [InSPIRE].

[48] S. Catterall, D.B. Kaplan and M. Ünsal, *Exact lattice supersymmetry*, *Phys. Rept.* **484** (2009) 71 [arXiv:0903.4881] [InSPIRE].

[49] A. Joseph, *Supersymmetric Yang-Mills theories with exact supersymmetry on the lattice*, *Int. J. Mod. Phys.* **A 26** (2011) 5057 [arXiv:1110.5983] [InSPIRE].

[50] G. Bergner and S. Catterall, *Supersymmetry on the lattice*, *Int. J. Mod. Phys.* **A 31** (2016) 1643005 [arXiv:1603.04478] [InSPIRE].

[51] S. Matsuura, T. Misumi and K. Ohta, *Topologically twisted N = (2, 2) supersymmetric Yang-Mills theory on an arbitrary discretized Riemann surface*, *PTEP* **2014** (2014) 123B01 [arXiv:1408.6998] [InSPIRE].

[52] S. Kamata, S. Matsuura, T. Misumi and K. Ohta, *Anomaly and sign problem in N = (2, 2) SYM on polyhedra: numerical analysis*, *PTEP* **2016** (2016) 123B01 [arXiv:1607.01260] [InSPIRE].

[53] S. Kamata, S. Matsuura, T. Misumi and K. Ohta, *Numerical analysis of discretized N = (2, 2) SYM on polyhedra*, PoS(LATTICE2016)210 (2016) [arXiv:1612.01968] [InSPIRE].

[54] M. Hanada and I. Kanamori, *Lattice study of two-dimensional N = (2, 2) super Yang-Mills at large-N*, *Phys. Rev.* **D 80** (2009) 065014 [arXiv:0907.4966] [InSPIRE].

[55] M. Hanada and I. Kanamori, *Absence of sign problem in two-dimensional N = (2, 2) super Yang-Mills on lattice*, *JHEP* **01** (2011) 058 [arXiv:1010.2948] [InSPIRE].

[56] I. Montvay, *Majorana fermions on the lattice*, hep-lat/0108011 [InSPIRE].

[57] H. Nicolai, *A possible constructive approach to (super-ϕ^3) in four-dimensions. 1. Euclidean formulation of the model*, *Nucl. Phys.* **B 140** (1978) 294 [InSPIRE].

[58] P. van Nieuwenhuizen and A. Waldron, *On Euclidean spinors and Wick rotations*, *Phys. Lett.* **B 389** (1996) 29 [hep-th/9608174] [InSPIRE].

[59] M. Lüscher and P. Weisz, *On-shell improved lattice gauge theories*, *Commun. Math. Phys.* **97** (1985) 59 [*Erratum ibid.* **98** (1985) 433] [InSPIRE].

[60] A.D. Kennedy, I. Horvath and S. Sint, *A new exact method for dynamical fermion computations with nonlocal actions*, *Nucl. Phys. Proc. Suppl.* **73** (1999) 834 [hep-lat/9809092] [INSPIRE].

[61] M.A. Clark and A.D. Kennedy, *The RHMC algorithm for two flavors of dynamical staggered fermions*, *Nucl. Phys. Proc. Suppl.* **129** (2004) 850 [hep-lat/0309084] [INSPIRE].

[62] M.A. Clark, P. de Forcrand and A.D. Kennedy, *Algorithm shootout: R versus RHMC*, PoS(LAT2005)115 (2006) [hep-lat/0510004] [INSPIRE].

[63] M.A. Clark, *The rational hybrid Monte Carlo algorithm*, PoS(LAT2006)004 (2006) [hep-lat/0610048] [INSPIRE].

[64] D. August, B. Wellegehausen and A. Wipf, *Spectroscopy of two dimensional $N = 2$ super Yang-Mills theory*, PoS(LATTICE2016)234 (2016) [arXiv:1611.00551] [INSPIRE].

[65] A. Donini, M. Guagnelli, P. Hernández and A. Vladikas, *Quenched spectroscopy for the $N = 1$ super Yang-Mills theory*, *Nucl. Phys. Proc. Suppl.* **63** (1998) 718 [hep-lat/9708006] [INSPIRE].

[66] D.J. Gross, I.R. Klebanov, A.V. Matytsin and A.V. Smilga, *Screening versus confinement in $(1 + 1)$-dimensions*, *Nucl. Phys.* **B 461** (1996) 109 [hep-th/9511104] [INSPIRE].

[67] A. Armoni, Y. Frishman and J. Sonnenschein, *Screening in supersymmetric gauge theories in two-dimensions*, *Phys. Lett.* **B 449** (1999) 76 [hep-th/9807022] [INSPIRE].

[68] M. Lüscher and P. Weisz, *Locality and exponential error reduction in numerical lattice gauge theory*, *JHEP* **09** (2001) 010 [hep-lat/0108014] [INSPIRE].

[69] B.H. Wellegehausen, A. Wipf and C. Wozar, *Casimir scaling and string breaking in G_2 gluodynamics*, *Phys. Rev.* **D 83** (2011) 016001 [arXiv:1006.2305] [INSPIRE].

[70] R. Sommer, *A new way to set the energy scale in lattice gauge theories and its applications to the static force and α_s in* SU(2) *Yang-Mills theory*, *Nucl. Phys.* **B 411** (1994) 839 [hep-lat/9310022] [INSPIRE].

[71] C. Morningstar and M.J. Peardon, *Analytic smearing of* SU(3) *link variables in lattice QCD*, *Phys. Rev.* **D 69** (2004) 054501 [hep-lat/0311018] [INSPIRE].

[72] S. Gusken, U. Low, K.H. Mutter, R. Sommer, A. Patel and K. Schilling, *Nonsinglet axial vector couplings of the baryon octet in lattice QCD*, *Phys. Lett.* **B 227** (1989) 266 [INSPIRE].

[73] UKQCD collaboration, *Gauge invariant smearing and matrix correlators using Wilson fermions at $\beta = 6.2$*, *Phys. Rev.* **D 47** (1993) 5128 [hep-lat/9303009] [INSPIRE].

[74] Y. Taniguchi, *One loop calculation of SUSY Ward-Takahashi identity on lattice with Wilson fermion*, *Phys. Rev.* **D 63** (2000) 014502 [hep-lat/9906026] [INSPIRE].

[75] S. Luckmann, *Ward-Identitäten in der $N = 1$ super-Yang-Mills-Theorie* (in German), Diplomarbeit, University of Münster, Münster, Germany (1997).

[76] T. Galla, *Supersymmetrische und Chirale Ward-Identitäten in einer diskretisierten $N = 1$-SUSY-Yang-Mills-Theorie* (in German), Diplomarbeit, University of Münster, Münster, Germany (1999).

[77] G. Munster, *The size of finite size effects in lattice gauge theories*, *Nucl. Phys.* **B 249** (1985) 659 [INSPIRE].

[78] M. Lüscher, *Volume dependence of the energy spectrum in massive quantum field theories. 1. Stable particle states*, *Commun. Math. Phys.* **104** (1986) 177 [INSPIRE].

[79] A.A. Migdal, *Recursion equations in gauge theories*, *Sov. Phys. JETP* **42** (1975) 413 [*Zh. Eksp. Teor. Fiz.* **69** (1975) 810] [INSPIRE].

[80] N.E. Bralic, *Exact computation of loop averages in two-dimensional Yang-Mills theory*, *Phys. Rev.* **D 22** (1980) 3090 [INSPIRE].

[81] S. Catterall, R. Galvez, A. Joseph and D. Mehta, *On the sign problem in* 2*D lattice super Yang-Mills*, *JHEP* **01** (2012) 108 [arXiv:1112.3588] [INSPIRE].

[82] S. Catterall, R.G. Jha, D. Schaich and T. Wiseman, *Testing holography using lattice super-Yang-Mills theory on a* 2*-torus*, *Phys. Rev.* **D 97** (2018) 086020 [arXiv:1709.07025] [INSPIRE].